



Contents lists available at ScienceDirect

Arabian Journal of Chemistry

journal homepage: www.sciencedirect.com



Original article

From ancient remedy to modern medicine: *Artemisia argyi* sesquiterpenoids as a promising natural treatment for COVID-19Yujing Huang^{a,b}, Zhilin Huang^a, YuHui Gan^a, Juntao Xie^a, Zhiyun Xia^a, Tao Liu^{d,e,f}, Xiangyu Chen^{d,e,f}, Xiangguang Li^a, Haibo Zhou^c, Pinghua Sun^c, Zhe Ren^{d,e,f,***}, Yifei Wang^{d,e,f,**}, Junxia Zheng^{a,b,*}^aSchool of Biomedical and Pharmaceutical Sciences, Guangdong University of Technology, Guangzhou 510006, China^bGuangdong Province Key Laboratory of Pharmacodynamic Constituents of TCM and New Drugs Research, Guangzhou 510006, China^cCollege of Pharmacy, Jinan University, Guangzhou 510632, China^dCollege of Life Science and Technology, Jinan University, Guangzhou 510632, China^eKey Laboratory of innovative technology research on natural products and cosmetics raw materials, Guangzhou 510632, China^f*Artemisia argyi* Lvl. et Van branch of National Engineering and Technology Research Center of Modernization of Traditional Chinese Medicine, Guangzhou 510632, China

ARTICLE INFO

Article history:

Received 15 May 2023

Accepted 20 September 2023

Available online 25 September 2023

Keywords:

Artemisia argyi Sesquiterpenes

COVID-19

UPLC-Q-Exactive-Orbitrap MS

Network pharmacology

ABSTRACT

Artemisia argyi H. Lévl. & Vaniot (*A. argyi*), a traditional Chinese herbal medicine, has been commonly used in plague epidemics and has bactericidal and sterilizing pharmacological effects. This study aimed to investigate the chemical composition and molecular mechanism of *A. argyi*, specifically focusing on its main active components, sesquiterpenoids. A total of 69 sesquiterpenoids were identified by UPLC-Q-Exactive-Orbitrap MS, of which 17 compounds were isolated. By integrating multiple databases, 91 overlapping protein targets were found between *A. argyi* sesquiterpenes and COVID-19, and 7 core targets and major signaling pathways for disease treatment were suggested. The techniques of SARS-CoV-2 pseudovirus (PsV) infection, fluorescence resonance energy transfer (FRET) and Surface plasmon resonance (SPR) have shown that some compounds in *A. argyi* can effectively inhibit PsV infection and the activities of M^{pro} and RBD and exert anti-inflammatory effects by reducing the secretion of NO. Molecular docking further confirmed the binding ability of these compounds to the corresponding proteins. It was found that Compound 10 (Achillinin C) could significantly inhibit the infection of PsV at a concentration of 14.85 μM, showing an anti-inflammatory effect and no obvious cytotoxicity to a variety of cells at this concentration. The study concludes that *A. argyi* holds promise as a natural treatment for COVID-19, offering multiple sesquiterpenoids with potential antiviral and anti-inflammatory properties. These findings provide a solid foundation for future research on traditional Chinese medicine for epidemic prevention.

© 2023 The Authors. Published by Elsevier B.V. on behalf of King Saud University. This is an open access article under the CC BY-NC-ND license (<http://creativecommons.org/licenses/by-nc-nd/4.0/>).

Abbreviations: *A. argyi*, *Artemisia argyi*; AASs, *Artemisia argyi* sesquiterpenes; ACE2, angiotensin converting enzyme2; Akt, protein kinase; DMSO, Dimethyl sulfoxide; Fr.6, fraction 6; Fr.8, fraction 8; FRET, fluorescence resonance energy transfer; GO, Gene Ontology; HIF-1, hypoxia inducible factor-1; HPLC, High-performance liquid chromatography; IL-6, interleukin 6; iNOS, inducible nitric oxide synthase; KEGG, Kyoto Encyclopedia of Genes and Genomes; LPS, Lipopolysaccharide; M^{pro}, Main protease; MTT, 3-(4,5-Dimethyl-2-thiazolyl)-2,5-diphenyl-2-H-tetrazolium bromide; NO, nitric oxide; ODS, Octadecylsilyl; PI3K, phosphoinositide 3-kinase; PPI, protein-protein interaction; PsV, Pseudovirus; RBD, Receptor Binding domain; SPR, Surface plasmon resonance; TLC, Thin-layer chromatography; TNF, tumor necrosis factor; TNF-α, tumor necrosis factor-alpha.

* Corresponding author at: School of Biomedical and Pharmaceutical Sciences, Guangdong University of Technology, China.

** Corresponding author at: College of Life Science and Technology, Jinan University, China.

*** Corresponding author at: College of Life Science and Technology, Jinan University, China.

E-mail addresses: rz62@163.com (Z. Ren), twang-yf@163.com (Y. Wang), junxiasheng@gdut.edu.cn (J. Zheng).

Peer review under responsibility of King Saud University.



<https://doi.org/10.1016/j.arabjc.2023.105298>

1878-5352/© 2023 The Authors. Published by Elsevier B.V. on behalf of King Saud University.

This is an open access article under the CC BY-NC-ND license (<http://creativecommons.org/licenses/by-nc-nd/4.0/>).

1. Introduction

Artemisia argyi H. Lévl. & Vaniot (*A. argyi*), also known as “Ai Hao”, “Qi Ai” and “Xiang Ai” in China, is a perennial plant species in the *Asteraceae* family that is commonly used in traditional medicine for its various health benefits. It is rich in active ingredients, including volatile oils, sesquiterpenoids, flavonoids, and polysaccharides, and shows a wide range of biological activities, including anti-inflammatory, anti-tumor, anti-oxidation, immune regulation, and so on (Liu et al., 2021). Meanwhile, sesquiterpenoids from *Artemisia* have been shown to have anti-inflammatory, anti-viral, anticancer and anti-oxidative effects (Shao et al., 2022, Sharifi-Rad et al., 2022, Wu et al., 2023). Sesquiterpenoids from *A. argyi* also exhibited anti-inflammatory effects by inhibiting MAPKs, NF- κ B, JNK/p38 and Jak2/Stat3 signaling pathways (Zeng et al., 2014, Li et al., 2023). Ancient Chinese books, such as “Wu Shi Er Bing Fang,” “Ling Shu,” and “Zhou Hou Bei Ji Fang,” document the use of *A. argyi* as a preventative measure against epidemics, where it was crushed and made into moxibustion strips and burned (Yang et al., 2021).

Moxibustion, a traditional Chinese cultural practice that has been passed down for thousands of years, has been shown to have unique advantages in preventing and treating SARS-CoV-2, such as relieving symptoms and preventing recurrence during the recovery

period (Liu et al., 2020, Wang et al., 2020, Guan et al., 2021), possibly by reducing the inflammatory response through its anti-inflammatory effects (Xu et al., 2020), as the volatile oil and sesquiterpenoids found in the burned moxibustion have been shown to be effective. Based on moxibustion intervention in COVID-19, it is necessary to study *A. argyi* volatile components, COVID-19 intervention and anti-inflammatory activity. While much research has focused on the volatile components of *A. argyi*, the sesquiterpenoids and their mechanism of treating pneumonia are not yet fully understood, thus further investigation is needed to elucidate the pharmacological basis of *A. argyi* sesquiterpenoids (AASs) and their therapeutic potential for pneumonia.

The SARS-CoV-2 spike protein plays an important role in viral entry (Yang et al., 2021). It is composed of two subunits, S1 and S2. The former can recognize and bind the host cell angiotensin converting enzyme2 (ACE2) receptor through receptor binding domain (RBD), and the latter can mediate the membrane fusion of spike protein (Hatmal et al., 2020, Fu et al., 2022, Liu et al., 2023). Among them, the affinity between the RBD of SARS-CoV-2 and ACE2 is 10 times higher than that of SARS-CoV RBD, indicating that RBD is an extremely important protein in the infection process (Muhseen et al., 2020). The development of SARS-CoV-2 entry inhibitors by targeting the RBD in the S1 subunit is an attractive strategy to inhibit viral entry and infection (Li et al., 2022). In all SARS-

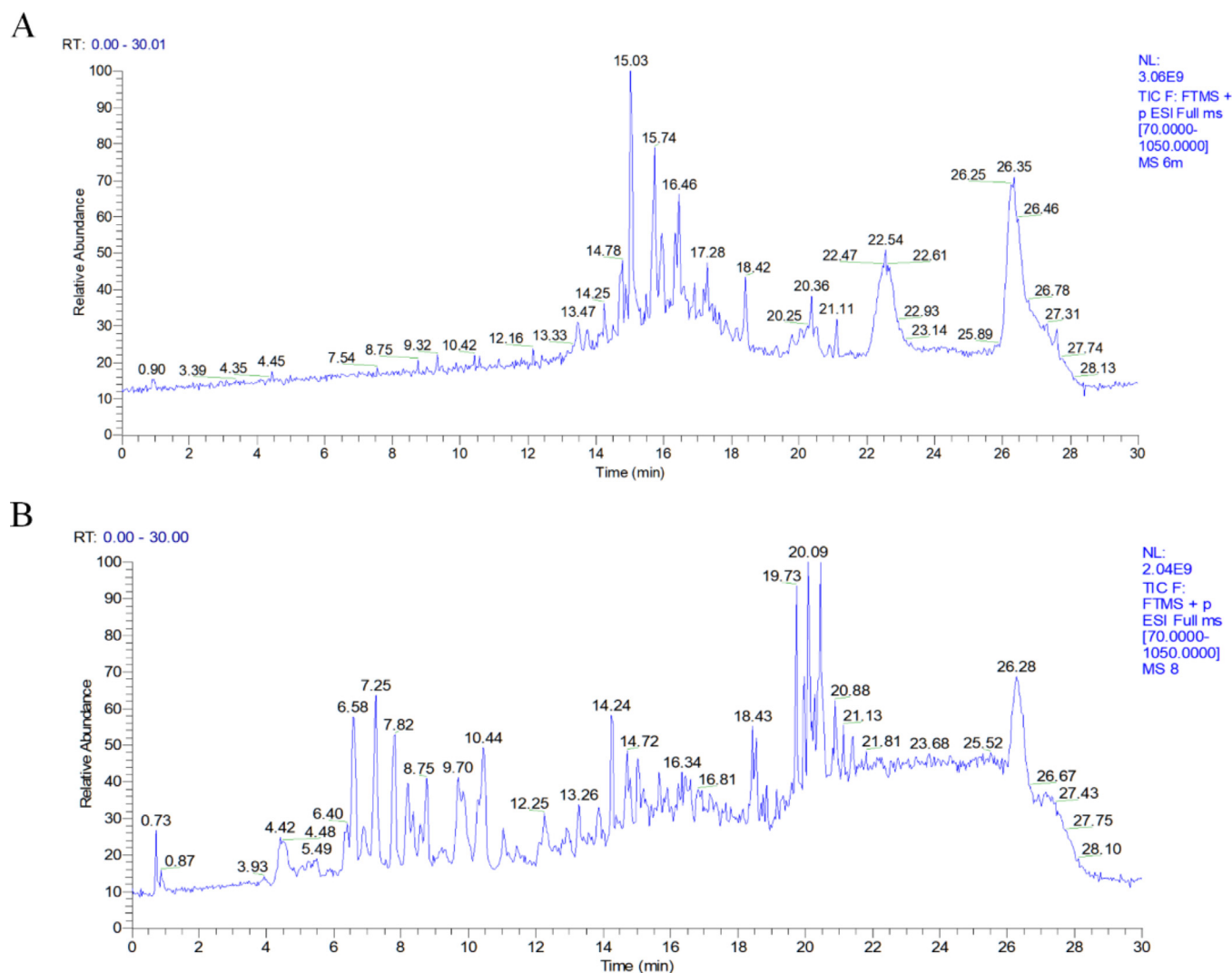


Fig. 1. The total ion chromatograms in positive ion modes of Fr.6 (A) and Fr.8 (B) in *A. argyi*.

CoV variants, main protease (Mpro) has undergone almost no mutations (Lee et al., 2022), and further deletion of its closely related homologus in humans has resulted in inhibitors having little on host cell proteases (V'Kovski et al., 2021, Lokhande et al., 2023). Therefore, mpro is necessary as one of the drug targets for effective inhibition of SARS-CoV-2 activity.

The complex chemical components in plant medicines make isolation and identification challenging, but the UPLC-Q-Exactive-Orbitrap MS technology, which combines chromatography and mass spectrometry, is a widely used and advantageous tool for analyzing complex plant drugs due to its high separation efficiency, fast scanning speed, high throughput, high resolution, and high sensitivity (Li et al., 2017, Wang et al., 2021). Additionally, network pharmacology, a systems biology-based network analysis of biological systems, can improve drug efficacy and reduce toxic side effects by regulating multiple signaling pathways, ultimately improving the success rate of clinical trials of new drugs and saving the cost of drug research and development (Wu et al., 2021). Because of the high risk in novel coronavirus, SARS-CoV-2 pseudovirus has become a key evaluation method in drug research and development (Chen and Zhang 2021). At the same time, anti-infective drugs largely rely on anti-inflammatory drugs to control the inflammatory factor storm of SARS-CoV-2 infection (Masih et al., 2021), and the choice of anti-inflammatory drugs often relies on Lipopolysaccharide (LSP) to stimulate stimulated RAW264.7 to secrete inflammatory mediators such as inducible nitric oxide synthase (iNOS) to catalyze inflammation (Bu et al., 2022, Park et al., 2022).

In this study, UPLC-Q-Exactive-Orbitrap MS and thin layer chromatography were used to screen total sesquiterpenoids from *A. argyi*, and AASs were purified by column chromatography using a variety of separation buffers. The isolated compounds were used to predict their therapeutic targets and molecular mechanisms for SARS-CoV-2 by network pharmacology. The compounds with anti-SARS-CoV-2 potential were screened by SARS-CoV-2 pseudovirus (PsV) infection, Surface plasmon resonance (SPR), FRET-based enzymatic assay, and the anti-inflammatory activity of the

compounds was evaluated by the inhibition of NO production in cells induced by LSP. The binding ability of the compounds to the corresponding proteins was evaluated by molecular docking. Finally, the effective antiviral and anti-inflammatory components in *A. argyi* were screened, which provided a solid foundation for the development and application of *A. argyi* and the future research on epidemic prevention of traditional Chinese medicine.

2. Materials and methods

2.1. Chemicals

The subject of this study was whole *A. argyi*, which was collected from Tangyin, Henan Province, China in May 2018. The plant was identified as *A. argyi* by Professor Wang Yifei of the College of Life Science and Technology, Jinan University.

95% EtOH (AR), petroleum ether (PE) (AR), ethyl acetate (EA) (AR), MTT powder, and DMSO were purchased from Zhiyuan Chemical Reagent Factory. Fetal bovine serum, DMEM high-glucose medium, PBS, and penicillin-streptomycin solution were purchased from Thermo Fisher Scientific; MeCN (HPLC grade) and MeOH (HPLC grade) were purchased from Oceanpak, Sweden. All other chemicals used were molecular biology grade.

2.2. Instrument conditions

High-performance liquid chromatography (HPLC) SHIMADZU LC 20AT/LC-6AD was purchased from Shimadzu (Japan), the Ultra Performance Liquid Chromatography Coupled with Q-Exactive Orbitrap Mass Spectrometry (UPLC-Q-Exactive-Orbitrap MS) was purchased from Thermo Fisher Scientific (China), Bruker amaZon SL low-resolution mass spectrometer was purchased from Brooke Dalton (USA), the rotary evaporator was purchased from EYELA (Tokyo, Japan), thin-layer chromatography silica gel plate was purchased from Merck (Germany), TD-low-temperature microextraction and concentration unit were purchased from Tianzhong Machinery Manufacturing Co., LTD (Wenzhou, China), and the sil-

Table 1
Mass spectral data of sesquiterpenes in Fr.6 from *A. argyi*.

No.	RT (min)	MS (error)	Fragment Ions	Formula	Identification	Rf
6-1	13.41	247.13231 [M + H] ⁺	229.1222, 201.1271, 173.0958	C ₁₅ H ₁₈ O ₃	α-Santonin	(Perez-Souto et al., 1992)
6-2	13.56	263.12845 [M + H] ⁺	245.1149, 234.9607	C ₁₅ H ₁₈ O ₄	Psilostachyin B	(Wang et al., 1993)
6-3	14.09	247.13228 [M + H] ⁺	229.1219, 264.1589, 269.1143	C ₁₅ H ₁₈ O ₃	Zedoalactone F	(Lou et al., 2009)
6-4	14.72	249.14798 [M + H] ⁺	231.1375	C ₁₅ H ₂₀ O ₃	(+)-Reynosin	(el-Feraly and Chan 1978)
6-5	14.86	303.08563 [M + H] ⁺	261.0738, 243.1009	C ₁₇ H ₁₈ O ₅	Dehydromatricarin	(Xue et al., 2021)
6-6	14.89	265.14050 [M + H] ⁺	173.0958, 145.1009, 131.0852	C ₁₅ H ₂₀ O ₄	Tauremisin	(Sheng et al., 2017)
6-7	15.03	271.12988 [M + Na] ⁺	231.1374, 145.1009	C ₁₅ H ₂₀ O ₃	Parthenolide	(Mathon et al., 2013)
6-8	15.16	251.16342 [M + H] ⁺	233.1533, 273.1457, 289.1196	C ₁₅ H ₂₂ O ₃	5(6)-Dihydroterrecyclic acid A	(Hirota et al., 1984)
6-9	15.49	231.13757 [M + H] ⁺	231.1271, 185.1322, 145.1009	C ₁₅ H ₁₈ O ₂	Dehydrocostus lactone	(Kallo et al., 2020)
6-10	15.49	271.05957 [M + Na] ⁺	253.1609	C ₁₅ H ₂₀ O ₃	7α-Hydroxyfrullanolide	(Ruangrungsi et al., 1989)
6-11	16.38	251.12485 [M + H] ⁺	233.0481, 223.0481	C ₁₅ H ₂₂ O ₃	11β, 13- Dihydrosantamarine	(Michalska et al., 2018)
6-12	16.45	265.14240 [M + H] ⁺	247.1691, 173.0958	C ₁₅ H ₂₀ O ₄	Zedoarofuran	(Li et al., 2015)
6-13	16.46	235.16872 [M + H] ⁺	217.1583, 137.0960, 95.0854	C ₁₅ H ₂₂ O ₂	(+)-Isopetasol	(Sumarah et al., 2010)
6-14	16.58	363.20816 [M + H] ⁺	321.1003, 303.0896	C ₂₀ H ₂₆ O ₆	Acanthospermolide	(Ganfon et al., 2012)
6-15	17.18	235.17935 [M + H] ⁺	235.1689, 124.1687	C ₁₅ H ₂₄ O ₃	2α,11-Dihydroxy-6-oxodrim-7-ene	(Liu et al., 2009)
6-16	17.20	335.18222 [M + H] ⁺	317.2098, 299.2003	C ₁₉ H ₂₆ O ₅	Arnicolide C	(Chan et al., 2019)
6-17	17.25	239.20020 [M + H] ⁺	221.1895, 203.1790	C ₁₅ H ₂₆ O ₂	llicol	(He et al., 2018)
6-18	17.27	233.15309 [M + H] ⁺	161.1321, 119.0855, 105.0700	C ₁₅ H ₂₀ O ₂	Isolantolactone	(Wang et al., 2021)
6-19	17.28	249.14977 [M-H] ⁻	231.1387	C ₁₅ H ₂₂ O ₃	A ₁	(Zdero et al., 1986)
6-20	17.28	257.15057 [M + H] ⁺	239.2002, 221.1895	C ₁₅ H ₂₈ O ₃	Eudesm-1β, 6α, 11-triol	(Song et al., 2014)
6-21	17.32	219.17392 [M + H] ⁺	201.1634, 191.1429	C ₁₅ H ₂₂ O	α-Cyperone	(Tine et al., 2017)
6-22	17.45	251.16509 [M-H] ⁻	233.1546, 207.1755	C ₁₅ H ₂₄ O ₃	Cyclobutanebutanoic acid	(Kanawati et al., 2008)
6-23	17.52	247.16710 [M + H] ⁺	229.1218, 211.1113, 183.1165	C ₁₅ H ₁₈ O ₃	Tourneforin	(Dzhalmakhanbetova et al., 2009)
6-24	17.52	235.16867 [M + H] ⁺	217.1583, 189.1634, 161.1322	C ₁₅ H ₂₂ O ₂	Artemisinic acid	(Ranasinghe et al., 1993)
6-25	17.62	221.18965 [M + H] ⁺	161.1323, 119.0855	C ₁₅ H ₂₄ O	(-)-Caryophyllene oxide	(Xiao et al., 2021)
6-26	17.65	219.17401 [M + H] ⁺	201.1635, 159.1166	C ₁₅ H ₂₂ O	Germacrone	(Razgonova et al., 2020)
6-27	17.90	351.18326 [M + H] ⁺	333.1728	C ₁₉ H ₂₆ O ₆	Arcotopicrin	(Hong et al., 2019)
6-28	19.61	297.23944 [M + H] ⁺	261.2547	C ₁₅ H ₂₀ O ₆	Isotanciloide	(Öksüz 1990)

*A₁ = 2-[(2S,4aR,8aS)-2-Hydroxy-4a-methyl-8-methylenedecahydro-2-naphthalenyl]acrylic acid.

ica gel column chromatography fillers (200–300 mesh) were purchased from Marine Chemical Works (Qingdao, China).

2.3. Extraction and isolation of sesquiterpenoids from *A. argyi*

A sample of *A. argyi* (2 kg) was weighed accurately and extracted with 95% EtOH three times for 24 h each at room temperature. The EtOH solution was filtered and concentrated in vacuum until dry, and the extract was dissolved in 1L of water. The extraction was repeated three times with an equal volume of PE and EA. The EA part was eluted with silica gel filler as the stationary phase and dichloromethane and methanol as the mobile phase according

to the ratio of 100:0, 99:1, 74:1, 64:1, 49:1, 33:1, 14:1, 9:1, 4:1, 1:1. All eluted parts were obtained with TLC and HPLC analysis, 9 components were obtained by combining them (Figure S1). Finally, according to the results of HPLC analysis, AASs were mainly enriched in Fr.6 and Fr.8 (Figure S2).

2.4. System conditions for UPLC-Q Exactive Orbitrap-MS

The AASs extract was prepared to a concentration of 1 mg/mL using methanol supplemented by ultrasonic dissolution, which was then filtered using 0.22 μm organic microporous filters.

Table 2

Mass spectral data of sesquiterpenes in Fr.8 from *A. argyi*.

No.	RT (min)	MS	Fragment Ions	Formula	Identification	Rf
8-1	7.24	301.10400 [M + Na] ⁺	243.1009, 215.1062	C ₁₅ H ₁₈ O ₅	11 β ,13-Dihydrodactucin	(Fan et al., 2016)
8-2	7.24	261.11157 [M + H] ⁺	243.1008, 173.0956	C ₁₅ H ₁₆ O ₄	Linderane	(He et al., 2018)
8-3	7.54	305.13528 [M + H] ⁺	179.7259	C ₁₇ H ₂₀ O ₅	Epoxydecompostin	(Yamakawa et al., 1981)
8-4	7.79	261.11041 [M + H] ⁺	243.1009, 225.0904, 215.1062	C ₁₅ H ₁₆ O ₄	14-Deoxylactucin	(Werner et al., 2003)
8-5	8.37	345.12997 [M + H] ⁺	284.1278, 266.4898	C ₁₉ H ₂₀ O ₆	Isoatriplicolide methylacrylate	(Wang et al., 2020)
8-6	8.41	231.13753 [M + H] ⁺	213.1270, 203.1433, 185.1321	C ₁₅ H ₁₈ O ₂	Atractylenolide I	(Ming et al., 2021)
8-7	8.76	297.08835 [M + H] ⁺	279.1216, 261.1114, 247.1322	C ₁₆ H ₂₄ O ₅	B ₁	(Cardona et al., 1992)
8-8	8.76	265.14290 [M + H] ⁺	247.1321, 229.1218	C ₁₅ H ₂₀ O ₄	Tanachin	(Triana et al., 2003)
8-9	8.76	247.13249 [M + H] ⁺	157.1008, 131.0854, 105.0699	C ₁₅ H ₁₈ O ₃	Tourneforin	(Talzhano et al., 2007)
8-10	9.73	279.12216 [M + H] ⁺	261.1115, 243.1009	C ₁₅ H ₁₈ O ₅	Urospermal A	(Zdero and Bohlmann 1990)
8-11	10.26	197.11676 [M + H] ⁺	179.1062	C ₁₁ H ₁₆ O ₃	Loliolide	(Calixto et al., 2016)
8-12	10.37	293.13742 [M + H] ⁺	261.1115, 247.1321	C ₁₆ H ₂₀ O ₅	3-O-methyl- isosecotanaparholide	(Öksüz 1990)
8-13	10.49	249.14702 [M + H] ⁺	231.1375, 213.1269, 185.1321	C ₁₅ H ₂₀ O ₃	2 α -Hydroxylantolactone	(Rustaiyan et al., 1991)
8-14	11.02	277.10809 [M-H] ⁻	233.1183	C ₁₅ H ₁₈ O ₅	Tanaphillin	(Vegh et al., 2018)
8-15	11.12	319.15091 [M + Na] ⁺	279.1581, 261.1115	C ₁₆ H ₂₄ O ₅	B ₂	(Adekenov et al., 1991)
8-16	11.41	281.19061 [M + H] ⁺	263.1268, 245.1166	C ₁₅ H ₂₀ O ₅	8 α -hydroxy-4-epi- sonchucarpolide	(Skaltsa et al., 2001)
8-17	11.44	263.12708 [M + H] ⁺	245.1166, 91.0545	C ₁₅ H ₁₈ O ₄	1-dehydroperuvinine	(Maldonado et al., 1985)
8-18	11.80	263.12698 [M + H] ⁺	245.1166, 235.1321	C ₁₅ H ₁₈ O ₄	Zederone epoxide	(Wang et al., 2014)
8-19	12.15	265.14255 [M + H] ⁺	247.1322, 229.1217	C ₁₅ H ₂₀ O ₄	3 α -hydroxyreynosin	(Hajdu et al., 2014)
8-20	12.24	281.13571 [M + H] ⁺	263.1269, 245.1165, 235.1324	C ₁₅ H ₂₀ O ₅	Xylaric acid D	(Yan et al., 2011)
8-21	12.54	245.11662 [M + H] ⁺	217.1219, 199.1113, 143.0853	C ₁₅ H ₁₆ O ₃	Inderalactone	(Wang et al., 2021)
8-22	12.85	263.12894 [M-H] ⁻	149.0972, 123.0816, 91.6389	C ₁₅ H ₂₀ O ₄	Artecalin	(Park et al., 2016)
8-23	13.25	261.11087 [M + H] ⁺	243.1009, 187.1114	C ₁₅ H ₁₆ O ₄	5 α -hydroxydehydroleucodin	(Li et al., 2017)
8-24	13.26	267.15631 [M + H] ⁺	249.1477, 231.1373, 213.1268	C ₁₅ H ₂₂ O ₄	Zedoalactone A	(Lin et al., 2020)
8-25	13.87	291.15573 [M + Na] ⁺	273.1461, 263.0798	C ₁₅ H ₂₄ O ₄	Ustusol A	(Liu et al., 2009)
8-26	14.01	307.15097 [M + H] ⁺	289.1414, 247.1323, 229.1218	C ₁₇ H ₂₂ O ₅	Perymeniolide	(Zdero and Bohlmann 1990)
8-27	14.14	315.09656 [M + H] ⁺	297.0879	C ₁₅ H ₁₉ O ₅ Cl	Chloroklotzchin	(Ahmed et al., 2003)
8-28	14.25	275.16107 [M + Na] ⁺	199.1119, 107.0712, 93.0372	C ₁₅ H ₂₄ O ₃	Zedoarondiol	(Liu et al., 2021)
8-29	14.65	291.15585 [M + Na] ⁺	273.1829, 245.0687	C ₁₅ H ₂₄ O ₄	Acoric acid	(Yalamanchili et al., 2017)
8-30	14.88	273.14523 [M + Na] ⁺	255.0897	C ₁₅ H ₂₂ O ₃	Hydroxyvalerenic acid	(Mathon et al., 2013)
8-31	14.91	565.23926 [M + Na] ⁺	547.2311, 319.1142, 301.1038, 269.1139	C ₃₀ H ₃₈ O ₉	Chrysanthemulide I	(Xue et al., 2018)
8-32	14.94	547.22906 [M + Na] ⁺	529.2176, 301.1039, 283.0933, 269.1147	C ₃₀ H ₃₆ O ₈	Artemisianins A	(Xue et al., 2019)
8-33	15.15	235.16866 [M + H] ⁺	189.1268, 175.1479, 147.1165	C ₁₅ H ₂₂ O ₂	Curcumenol	(Liu et al., 2021)
8-34	15.17	237.10933 [M + H] ⁺	219.1738, 201.1634	C ₁₅ H ₂₄ O ₂	B ₃	(Garlaschelli and Vidari 1989)
8-35	15.38	299.20016 [M + H] ⁺	281.1352, 263.1613, 220.9056	C ₁₅ H ₂₂ O ₆	Hydroheptelidic acid	(Nielsen et al., 2011)
8-36	15.80	291.15607 [M + Na] ⁺	203.1037	C ₁₅ H ₂₄ O ₄	Ustusol B	(Xu et al., 2020)
8-37	15.90	251.12477 [M + H] ⁺	233.1159, 123.3146	C ₁₅ H ₂₂ O ₃	7-Hydroxypetasol	(Sugawara et al., 1993)
8-38	16.14	237.14566 [M + H] ⁺	269.1741, 219.1737, 201.1636	C ₁₄ H ₂₀ O ₃	B ₄	(Sugawara et al., 1993)
8-39	16.75	265.14026 [M + H] ⁺	297.2042, 247.1321, 229.1213	C ₁₆ H ₂₄ O ₃	12-Methoxydihydrocostunolide	(Mathon et al., 2013)
8-40	16.89	277.17676 [M + Na] ⁺	309.2029, 245.1506	C ₁₅ H ₂₆ O ₃	B ₅	(Velten et al., 1994)
8-41	17.09	253.14015 [M + H] ⁺	235.1684, 217.1581, 189.1633	C ₁₅ H ₂₄ O ₃	Illicic acid	(Jimenez-Gonzalez et al., 2018)
8-42	17.73	261.11087 [M + Na] ⁺	243.1009	C ₁₅ H ₂₆ O ₂	11,12-Dihydroxydrimene	(Velten et al., 1994)

* B₁ = Methyl (1R,2R,3R,4S,6S)-4-ethenyl-2,6-dihydroxy-3-[1-(hydroxymethyl) ethenyl]-4-methyl- α -methylene-cyclohexaneacetate; B₂ = 6 α -Acetoxy-13-methoxy-1 ~ 10:4t5-diepoxysermacr-8,10-olide; B₃=(4S,4aR,8aS)-4a,5,6,7,8,8a-Hexahydro-4-(hydroxymethyl)-3,4a,8,8-tetramethyl-1(4H)-naphthalenone; B₄ = 3-(2-methyl-3-oxo-1,2,3,5,6,7,8,8a-octahydronaphthalen-1-yl)propanoic acid; B₅=(1,6-dimethyl-1,3,4,5,8,8a-hexahydronaphthalene-1,4a,5(2H)-triyli)trimethanol.

Fr.6 and Fr.8 of *A. argyi* were separated on a Hypersil GOLD C18 (100 × 2.1 mm, 1.9 μm) column at a flow rate of 0.3 mL/min, injection volume of 2 μL, and column temperature of 40° C. The mobile phase consisted of 0.1% formic acid aqueous solution (phase A) and methanol solution (phase B). Gradient elution: 0.01–10.00 min, 10–30% B; 10.00–18.00 min, 30–95% B; 18.00 to 24.00 min, 95% B; 24.00 ~ 26.00 min, 95–10% B; 26.00 to 30.00 min, 10% B.

The high-resolution MS source parameters used in this study comprised + 4.0kV and –3.0kV spray voltage, 30arb sheath gas, 10arb auxiliary gas, 0 purge gas, 320 °C ion transfer tube temperature, and 350 °C auxiliary gas heating temperature, and were detected in positive and negative ion modes. The molecular formula and exact molecular weight of the primary mass spectrum were determined using Compound Discoverer 3.2 software and matched with both the mzCloud network database and a local traditional Chinese medicine component database. The data were further analyzed using mass spectrometry software and compound database for comparison.

2.5. Extraction and isolation

Subsequently, the compounds were isolated by silica gel column chromatography, ODS column chromatography and prepara-

tive high performance liquid chromatography (HPLC) (Chen et al., 2022). 17 compounds were obtained with a purity of greater than 95% and dissolved in DMSO at 4 °C (Xia et al., 2023). The specific purification process is shown in Figure S2.

2.6. Target collection and network pharmacology analysis

The chemical components in this study were derived from the extraction and isolation of *A. argyi*. The target gene set of *A. argyi* was obtained by searching several databases: (1) CTD (<https://ctdbase.com/>); (2) SwissTargetPrediction server (<https://www.swiss-targetprediction.ch>); (3) SuperPred (<https://prediction.charite.de/>). Target to obtain from GeneCards database (<https://www.genecards.org/>) to select 400 protein targets. Finally, Cytoscape will be used to collect the targets for “compaction-target-disease” mapping.

2.7. Bioinformatics analysis of AASs

To enhance the understanding of drug efficacy, the core targets of COVID-19 associated AASs were incorporated into STRING for Protein-protein interaction (PPI) analysis. Interaction networks were constructed using PPI data with a confidence score above

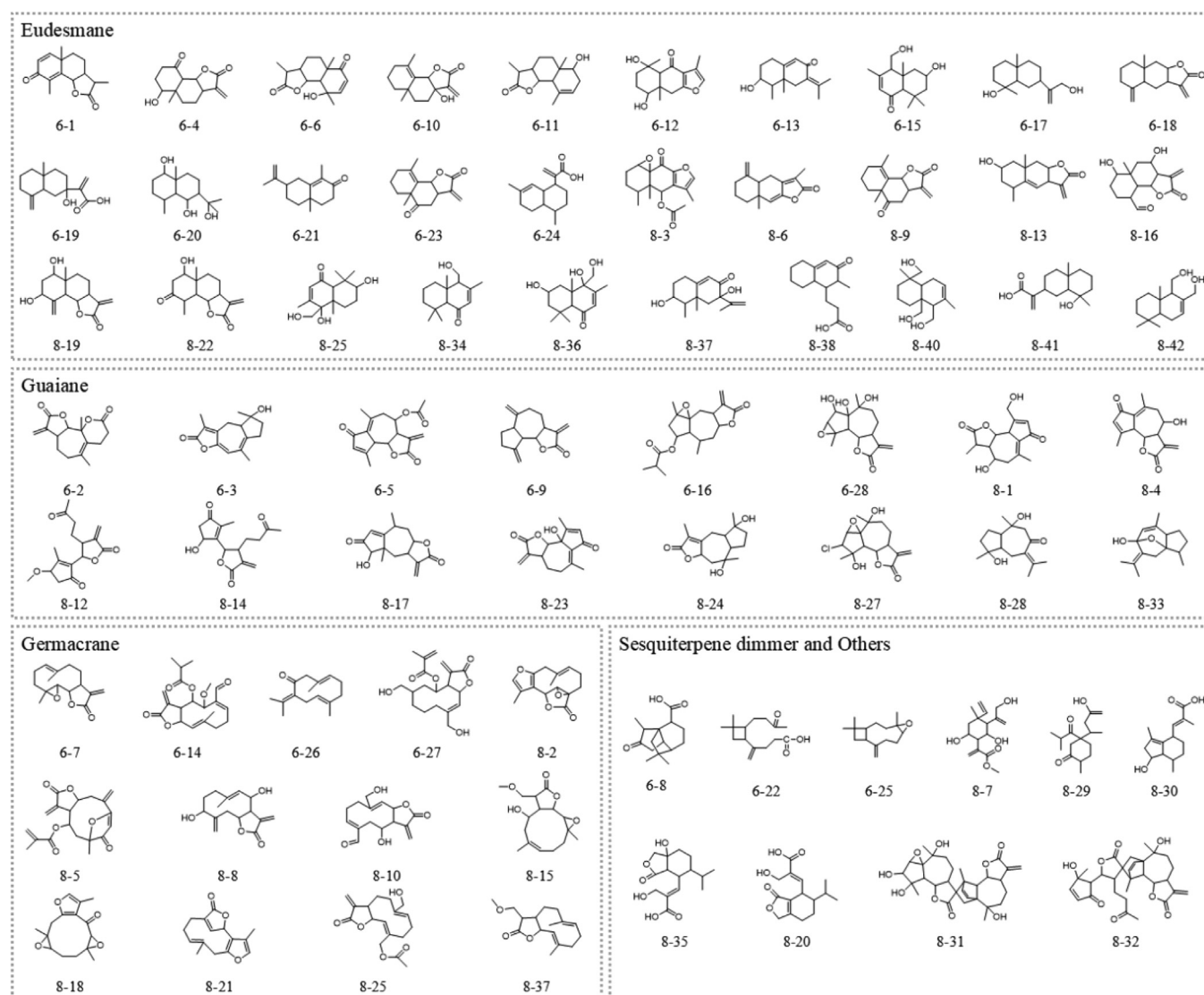


Fig. 2. Structure of sesquiterpenoids in *A. argyi*.

0.9, and hub genes were identified to perform functional enrichment through KEGG pathway and GO analyses, which were visualized using Metascape (<https://metascape.org>) and DAVID (<https://david.ncifcrf.gov>) combined with the R package cluster Profiler (version 4.2.1) (Wang et al., 2022). Only pathways or terms with an adjusted p-value < 0.05 and q-value < 0.01 were deemed significant.

2.8. SARS-CoV-2 M^{Pro} activity assay

The activity of SARS-CoV-2 M^{Pro} was measured using a fluorescence resonance energy transfer assay in a 96-well black flat plate. The reaction volume was 100 μL per well and consisted of 90 μL of assay buffer, 1 μL of 2019-nCoV M^{Pro}/3CL^{Pro}, 4 μL of substrate (Dabcyl-KTSAVLQSGFRKME-Edans) (Beyotime Company, China),

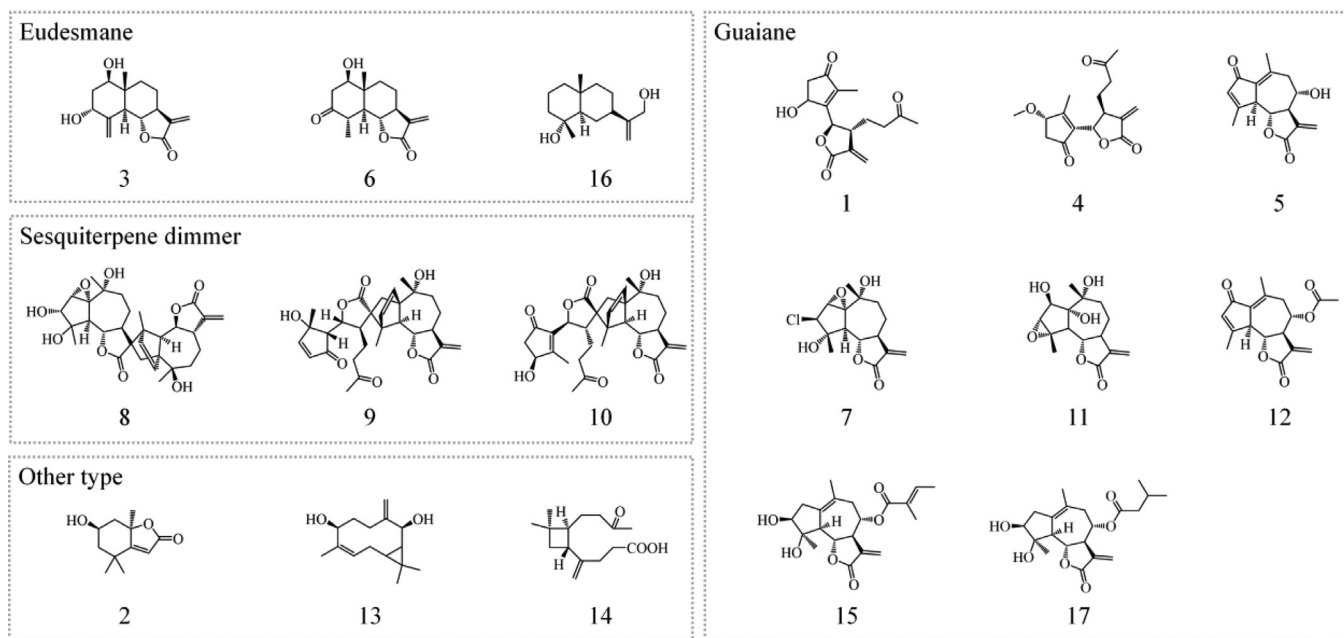


Fig. 3. Compounds isolated from Fr.6 and Fr.8 in *A. argyi*.

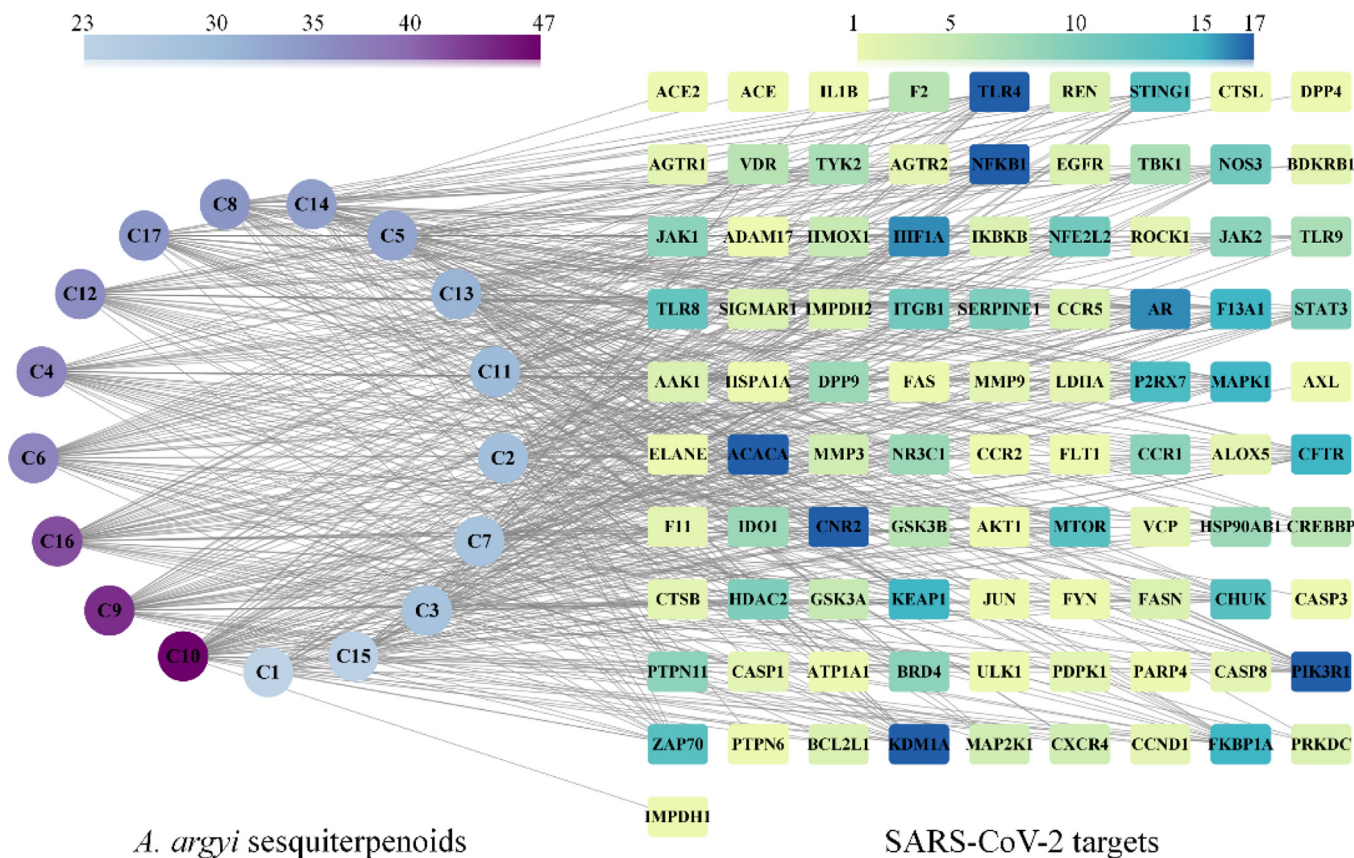


Fig. 4. Compound-target network of *A. argyi* sesquiterpenoids formula constructed using Cytoscape.

and 5 μL of AASs at various concentrations (dissolved in DMSO). The concentrations of Ebselen were 0.08, 0.16, 0.31, 0.63, 1.25, 2.50, 5.00, and 10.00 μM , while those of AASs were 2.5, 5, 10, and 20 μM . The blank control well contained 91 μL of assay buffer, 5 μL of DMSO, and 2 μL of substrate. The enzyme activity control well contained 92 μL of detection buffer, 1 μL of M^{pro} , 5 μL of DMSO, and 4 μL of substrate, and the sample well contained 90 μL of detection buffer, 1 μL of M^{pro} , 5 μL of DMSO, and 4 μL of substrate. The plate was incubated in darkness at 37 $^{\circ}\text{C}$ for 5 min, and the fluorescence signal was measured using a multi-scan spectroscopy (Thermo Fisher, Shanghai, China) with excitation/emission wavelengths of 325/393 nm. The results were quantified using Formula 1.

$$\text{Inhibitionrate}(\%) = \frac{(RFU_{100\% \text{enzyme activity control}} - RFU_{\text{sample}})}{(RFU_{100\% \text{enzyme activity control}} - RFU_{\text{blank control}})} \times 100\% \quad (1)$$

2.9. Surface plasmon resonance (SPR) assay

The RBD (Sino Biological, 40592-V05H) was immobilized on a CM5 sensor chip using an amino coupling reaction, with PBS-P + used as the running buffer. The RBD was diluted to a final concentration of 25 $\mu\text{g}/\text{mL}$ using a sodium acetate solution (10 mM,

pH 4.5) and the immobilization level was around 9700 RU (Response Units). To perform the binding assays, AASs were diluted in 5% DMSO PBS-P + running buffer to concentrations of 200 μM , 100 μM , 50 μM , 25 μM , 12.5 μM , 6.25 μM , and 3.125 μM , and then passed over the sensor chip at a flow rate of 30 $\mu\text{L}/\text{min}$ for 60 s. The dissociation time was 60 s. The data were analyzed using the Biacore evaluation software, and the K_D values were calculated by either kinetic analysis or steady-state affinity method (Yi et al., 2022).

2.10. Cell culture

HEK293T, HEK293T/ACE2, RAW264.7, HepG2, A549 and Caco-2 cell lines were cultured in Dulbecco's Modified Eagle Medium (DMEM, Gibco, USA) supplemented with 10% fetal bovine serum (FBS, Capricorn scientific, Germany) and 1% penicillin (100 units/ml)/streptomycin (100 $\mu\text{g}/\text{mL}$) (Gibco, USA). 293T cells stably expressing human-ACE2 (293T/ACE2) were constructed by our laboratory.

2.11. Cell viability

HEK293T/ACE2, RAW264.7, HepG2, A549, and Caco-2 cells were seeded in 96-well plates at 5000 cells per well. After 24 h, the complete medium was removed, and 100 μL of DMEM solution con-

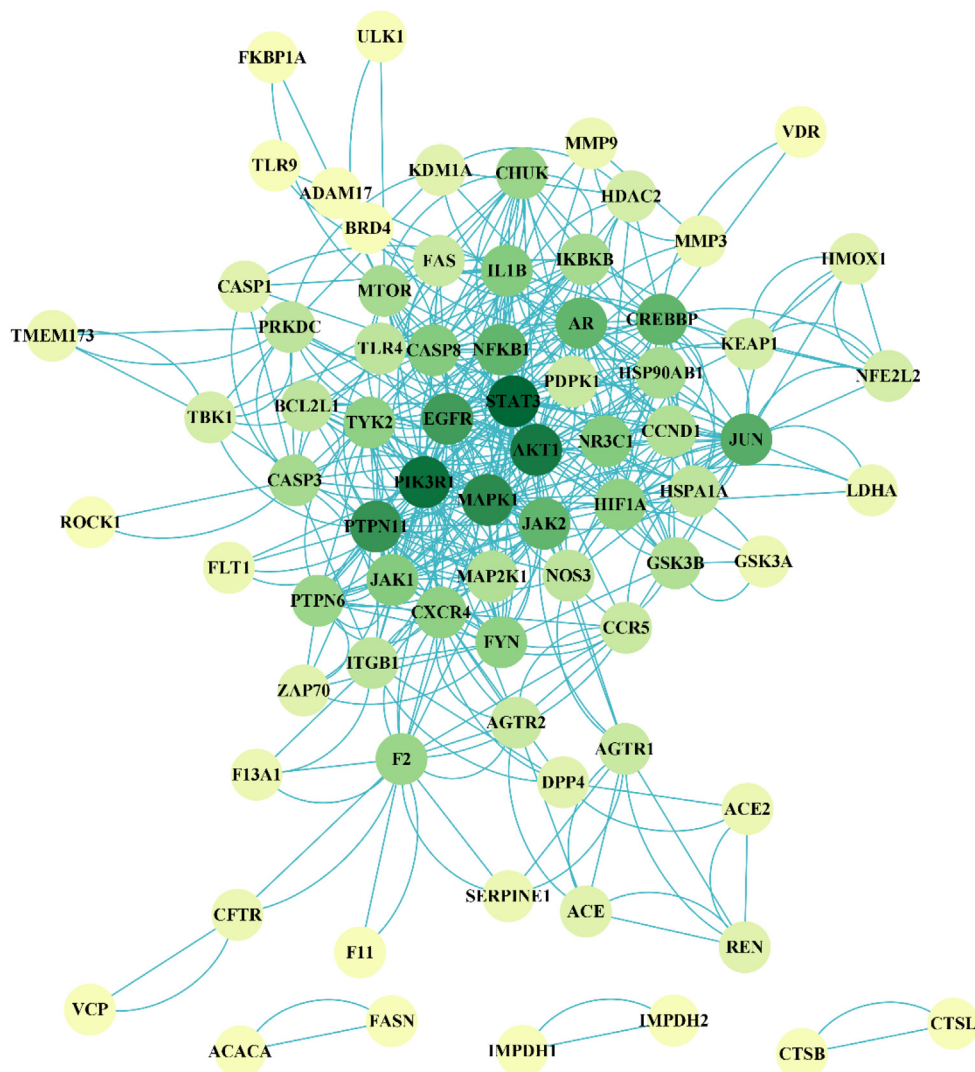


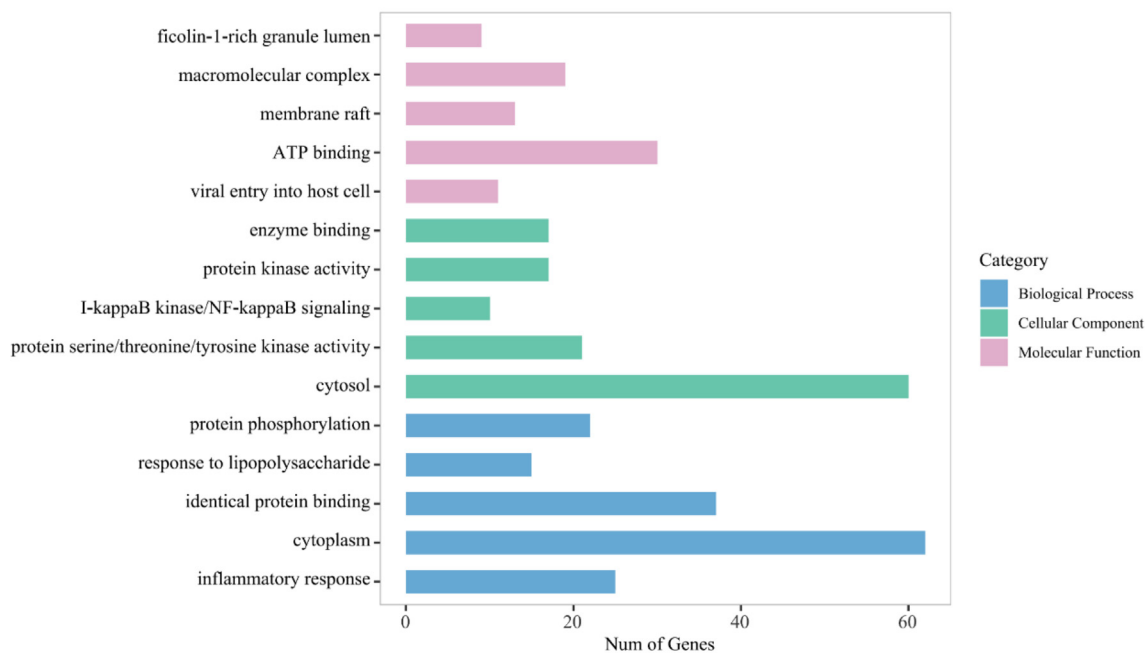
Fig. 5. PPI of AASs in treating COVID-19.

taining AASs at different gradient concentrations was added, and the culture was continued for 48 h. Cell viability was examined by an MTT colorimetric assay. Briefly, 10 μ L 0.5 mg/mL MTT [3-(4,5-dimethylthiazol-2-yl)-2,5-diphenyltetrazolium bromide] (Sigma-Aldrich) was added to each well and incubated for 4 h in an incubator. The medium was then replaced with DMSO (Macklin, Shanghai, China) to dissolve the formazan crystals (Sa-Ngiamsumtorn et al., 2021). Absorbance was measured at a wavelength of 570 nm on a microplate reader (Thermo Fisher).

2.12. SARS-CoV-2 pseudovirus (PsV) infection assay

The pCDNA3.1(+)-2019-HnCoV-Spike(SARS-Cov-2), pVSV-G, and pNL4-3-Luc-R-E- plasmids (MiaoLingBio, Wuhan, China) were co-transfected into HEK293T cells to package SARS-CoV-2 PsV (Xia et al., 2020, Li et al., 2021). The supernatant containing PsV was collected at 48 h after transfection, centrifuged at 3000 g for 10 min, filtered and stored at -80°C . To evaluate the inhibitory activity of AASs against PsV infection, 293T/ACE2 cells (5000 cells

A



B

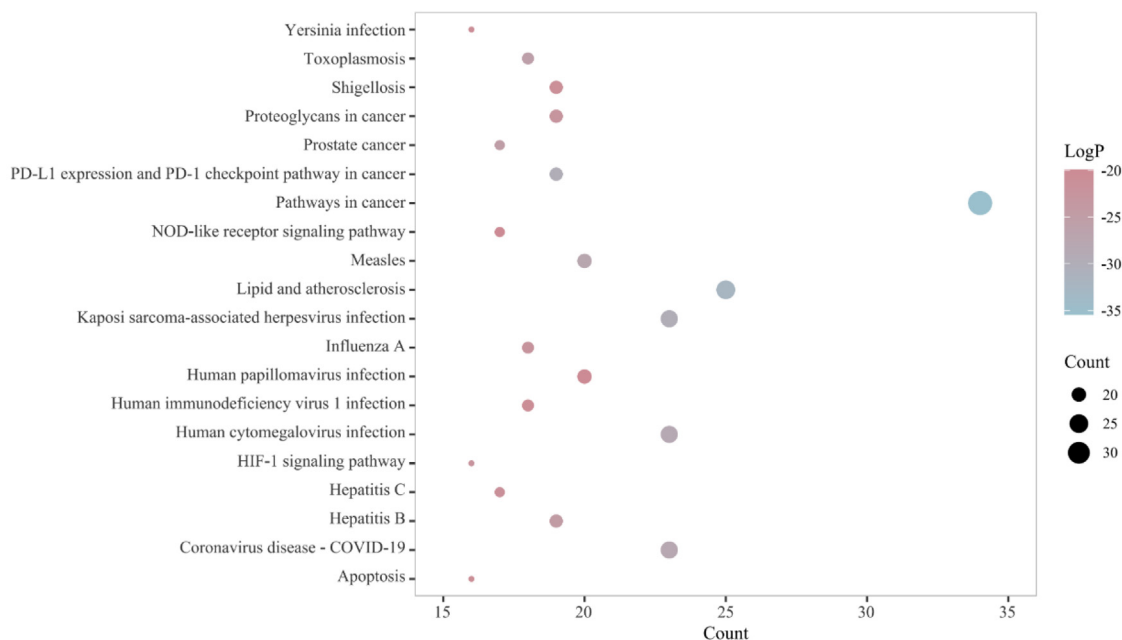


Fig. 6. (A) The top 5 pathways for GO enrichment analysis of the targets of AASs. (B) The top 20 pathways for KEGG enrichment analysis of the targets of AASs.

/ well) were seeded into 96-well plates and cultured at 37 °C in 5% CO₂. After 24 h, 50 μL of gradient concentrations of AASs compounds and 50 μL of PsV supernatant were added to each well and mixed and incubated with the cells for 72 h. Remove medium, PBS washing, and use with 100 mM potassium phosphate buffer (pH 7.8), 0.2% of Triton X - 100, and 1 mM DTT splitting cells (Wu et al., 2019). After full lysis, 20 μL of cell lysate was added to a white 96-well plate, and 80 μL of reaction substrate (1 mM ATP, 5 mM MgSO₄ and 0.5 mM D-Luciferin) was added, and the luminescence reaction was quantitatively measured in a 96-well microplate photometer. The inhibition rate of PsV was calculated as shown in Formula 2.

$$\text{Inhibition rate (\%)} = \frac{(C_{\text{solvent blank}} - C_{\text{sample}})}{(C_{\text{solvent blank}} - C_{\text{group without PsV}})} \times 100\%. \quad (2)$$

2.13. Determination of nitric oxide content in RAW 264.7 cells induced by LPS

In order to study the anti-inflammatory activity of *A. argyi*, the anti-inflammatory activity of 17 compounds was evaluated in lipopolysaccharide (LPS)-induced RAW264.7 cell inflammation model in vitro (Masih et al., 2021). Cells were cultured in 24-well plates at 2×10^5 cells per well for 24 h. The medium was removed and 400 μL of various concentrations of AASs were added. After 2 h of AASs treatment, 4 μL of 0.1 mg/mL LPS solution (dissolved in PBS) was added to the model group and the experimental group, and 4 μL of PBS was added to the blank group for 24 h. 50 μL of the supernatant from each well of a 24-well plate was transferred to a 96-well plate and the Griess kit (Beyotime Company, China)

was added to determine the NO content (Xue et al., 2021). Absorbance values were measured at a wavelength of 562 nm using a microplate reader, and nitric oxide concentration was calculated from a standard curve, as shown in Formulae 3.

$$y = 170.6334x - 7.0236 \quad (3)$$

2.14. Molecular docking

Through SPR, enzyme inhibition experiments and anti-inflammatory activity screening, it was found that AASs could closely bind to the RBD of SARS-CoV-2, effectively inhibit the enzyme activity of M^{Pro}, and effectively inhibit the production of NO by inflammatory cells. However, the structure-activity relationships between these compounds and their corresponding proteins are not yet.

ChemOffice 2019 was utilized to draw the structures of AASs, while Autodock 4.2.6 was employed to optimize these compounds. The protein structures of SARS-CoV-2 RBD (PDB ID: 6m0j), COVID-19 M^{Pro} (PDB ID: 6LU7), and iNOS (PDB ID: 4CX7) were processed using Pymol and imported into Autodock for docking. The binding sites between small molecules and proteins were determined based on previous studies, and for RBD, the binding site was located between RBD and ACE2. A grid box with dimensions of 60 Å × 60 Å × 60 Å and grid spacing of 0.375 Å was centered at (x = -34.527, y = 20.545, z = 10.113). For COVID-19 M^{Pro}, the grid box was set according to the location of its receptor, with dimensions of 40 Å × 40 Å × 40 Å, coordinates of (x, y, z) of -9.253, 16.459, 65.388, and grid spacing of 0.375 Å (Ye et al., 2021). The iNOS binding site was defined by a grid box centered on the co-

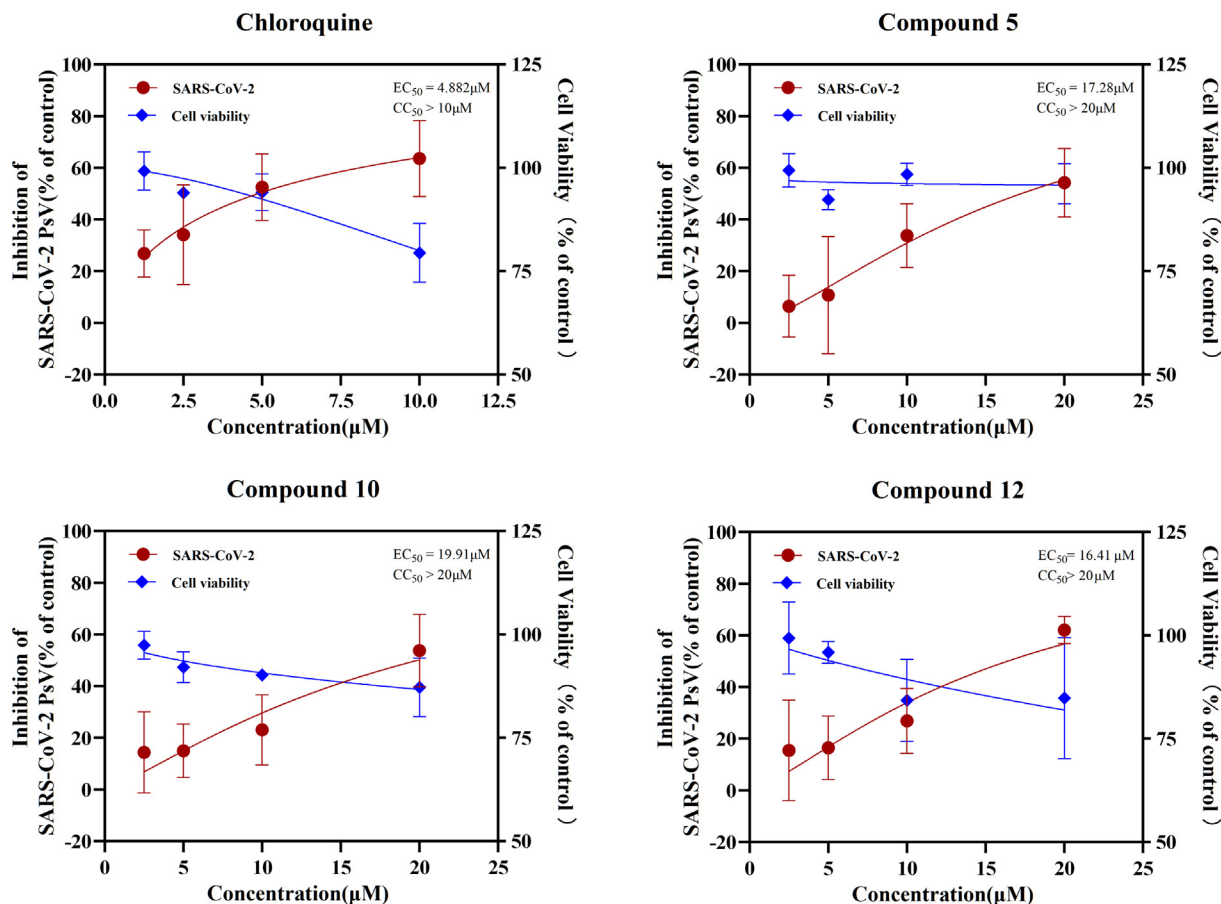


Fig. 7. Inhibitory activity of the positive drugs chloroquine, Compound 5, 10 and 12 against pseudovirus infection in HEK293T/ACE2 cells.

crystallization inhibitor ($x = -11.594$, $y = -60.255$; $z = 15.846$) with dimensions of $40 \text{ \AA} \times 40 \text{ \AA} \times 40 \text{ \AA}$ and mesh spacing of 0.375 \AA .

The processed ligands and receptors were imported into AutoDock 4.2.6 and molecular docking was performed using default parameters. Finally, the docking results were analyzed and processed using PyMol 2.5, ligplot⁺ 2.2.5 and Chimera 1.16.

2.15. Data statistics

Experimental data are presented as mean \pm SD, and all grouped data were statistically analyzed using Graphpad Prism 8.4.3 software. When $P < 0.05$ was considered statistically significant. Significant differences between data from each group were assessed by ANOVA.

3. Results

3.1. Analysis results of UPLC-Q-Exactive-Orbitrap-MS

Fr.6 and Fr.8 in the positive ion mode of the sagitta sesquiterpene extract are depicted in Fig. 1, which display the total ion cur-

rent signals. By comparing the primary mass spectrum information, fragmentation, and molecular formula of compounds reported in relevant literature, and combining the matching compounds from mzCloud and mzVault databases, a total of 28 and 42 terpenoids were preliminarily identified in Fr.6 and Fr.8, respectively (Table 1 and Table 2). The structure diagram is illustrated in Fig. 2. The identified sesquiterpenes included 16 guaiacane, 30 eucalane, 13 gemmarane, and 8 other sesquiterpenes, as well as 2 sesquiterpene dimers and one monoterpenoid.

3.2. Structural identification of *A. argyi* compounds

17 compounds were isolated from *A. argyi* by various chromatographic methods, and their structures were determined as Tanaaphilin (1), Loliolide (2), 3α -hydroxyryanosin (3), 3-methoxytanaphthole (4), 14-deoxyylactin (5), Artecain (6), Chlorofluotzchin (7), Chrysanthemulide I (8), Artemisianins A (9), Achillinin C (10), Isotanciloide (11), Dehydromatricarin A (12), *epi*-Baynol A (13), 3, 3-Dimethyl- γ -methylene-2-(3-oxobutyl) cyclobutanoic acid (14), Arginin C (15), Ilicic alcohol (16), Arginin A (17), through extensive spectra analysis (Fig. 3).

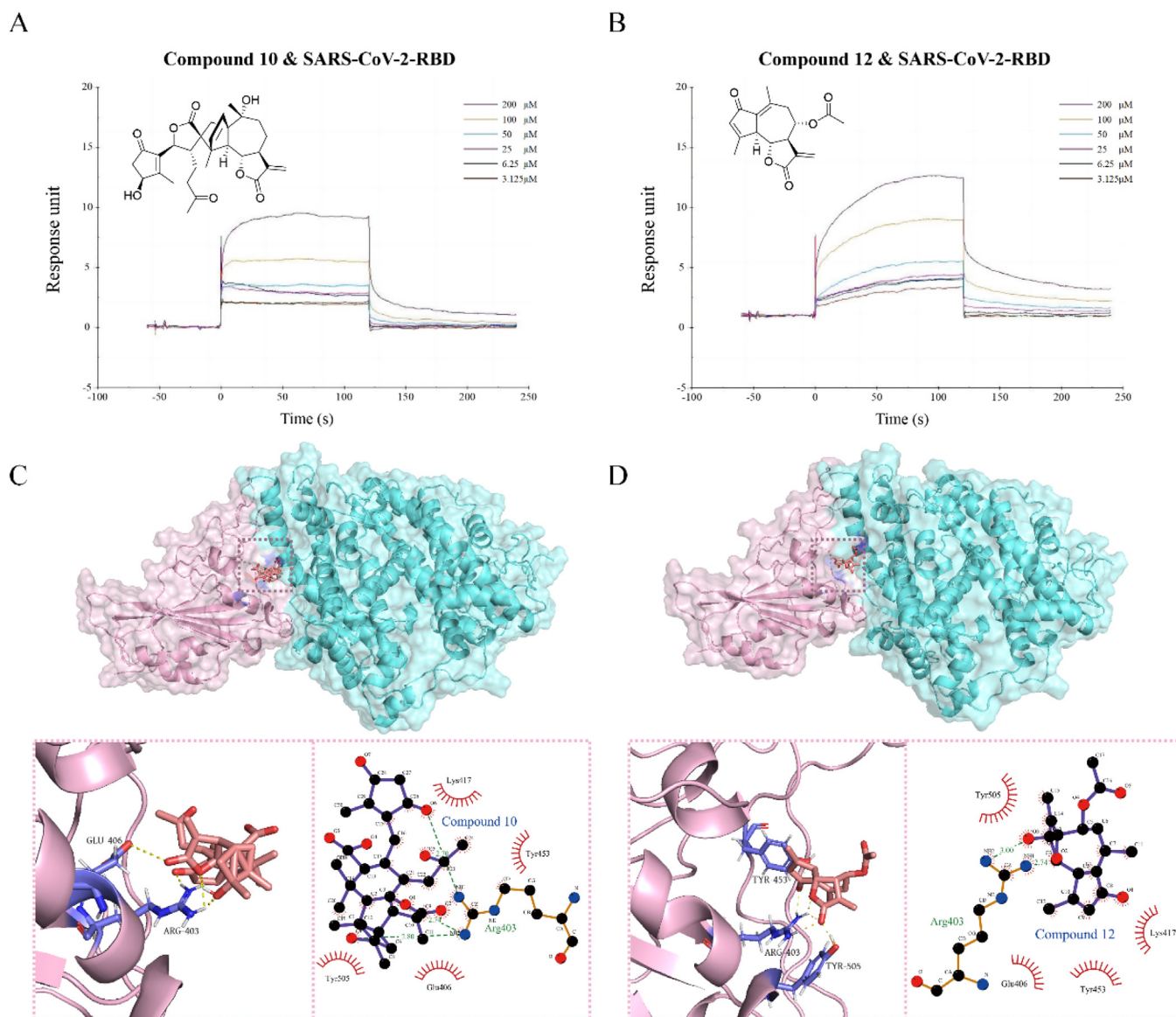


Fig. 8. The molecular interaction of RBD and C10(A) and C12(B). The molecular interaction of RBD and C10(C) and C12(D).

3.3. Target collection of active ingredients of AASs

17 sesquiterpenoids isolated from *A. argyi* were identified using CTD, SwissTargetPrediction server and SuperPred, and 806 protein targets were predicted. In addition, 400 targets of "COVID-19" and "SARS-CoV-2" were obtained from GeneCard database, and 275 targets of SARS-CoV-2 were selected. 91 of these targets overlapped with AASs. Cytoscape was used to generate a drug-target-disease map (Table S1). The "drug-target-disease" diagram was generated using Cytoscape (Fig. 4). Compounds 10, 9, 16, 6, 4 and 12 showed more than 35 cross-protein targets with SARS-CoV-2, suggesting their potential therapeutic effects. Notably, AASs targeted key proteins such as NFKB1, ACACA, CNR2, KDM1A, TLR4 and PIK3R1 in treatment.

The PPI of intersection targets was obtained by String database and visualized by Cytoscape (Fig. 5). The average degree of each protein was 12.84, with 29 protein targets having nodes greater than the average, while STAT3, PIK3R1, AKT1, MAPK1, PTPN11, EGFR, and JUN had nodes greater than 30, indicating that these 7 targets are the core targets of AASs for the treatment of COVID-19.

3.4. GO biological function annotation and KEGG pathway enrichment analysis

Functional enrichment analysis of GO and KEGG was performed to investigate the potential mechanism of AASs in the treatment of SARS-CoV-2. For example, molecular functions mainly include ATP binding and viral entry into host cell, AASs involve cellular compo-

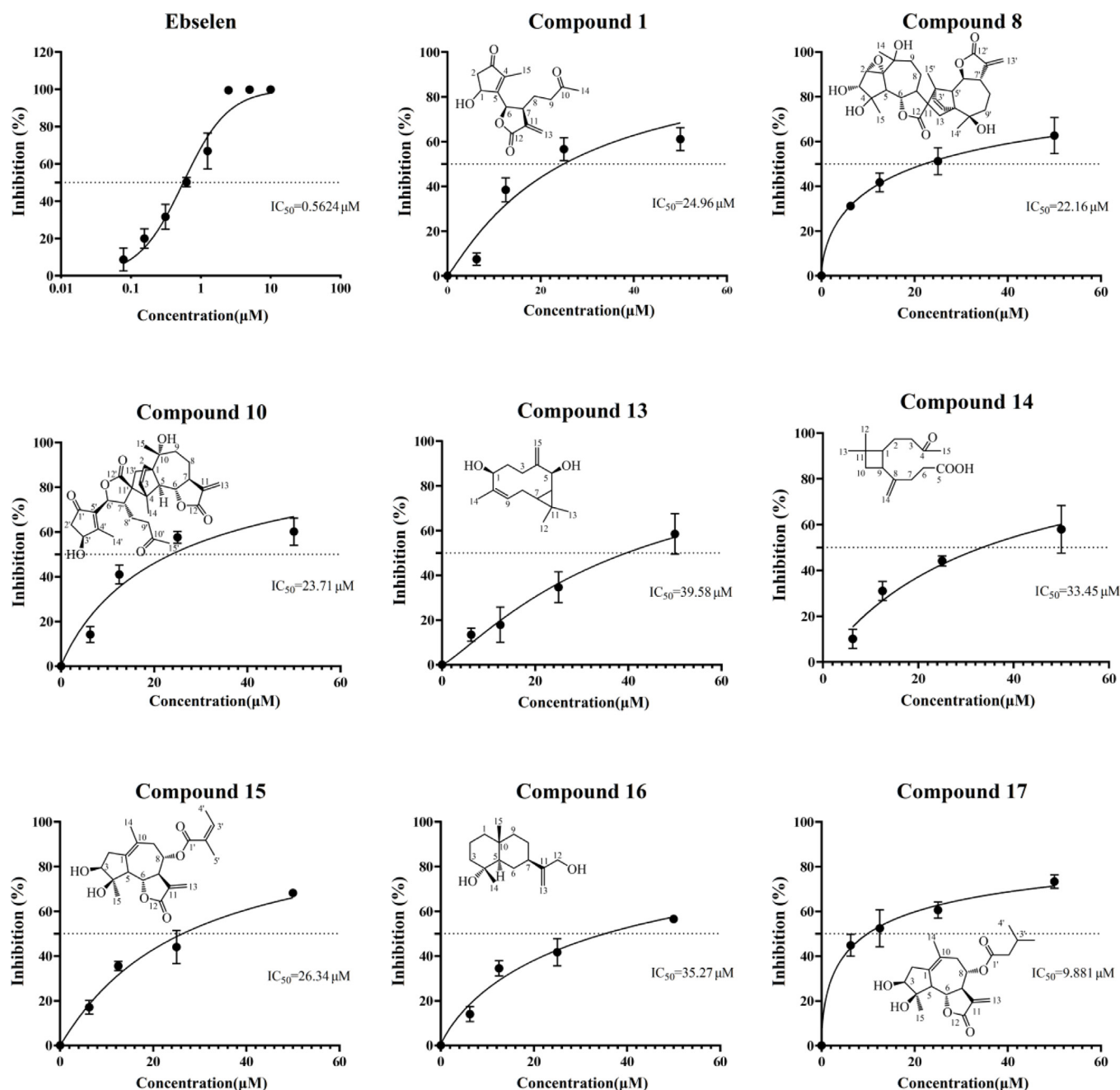


Fig. 9. (A) Protease activities of SARS-CoV-2 M^{Pro} in the presence of inhibitors were measured by FRET-based enzymatic activity assay. IC₅₀ of Ebselen and Compounds 1, 8, 10, 13, 14, 15, 16 and 17.

nents including cytoplasm, and biological processes include the response to lipopolysaccharide, inflammatory response, and so on (Fig. 6(A)). The top 20 results obtained by KEGG pathway analysis are shown in Fig. 6(B), indicating the proportion of target genes belonging to a certain pathway to all annotated genes in the pathway, with dot size representing the number of target genes. The analysis revealed that a majority of the diseases associated with the identified targets were viral-related, with pathways in cancer being the most prevalent. This suggests that AASs may have potential involvement in multiple cancer-related pathways for treatment purposes. Furthermore, the NOD-like receptor and HIF-1 signaling pathways were identified as the primary signaling pathways targeted by AASs in relation to COVID-19.

3.5. Analysis of anti-pseudovirus infection

To screen for potential inhibitors of SARS-CoV-2 entry in *A. argyi*, pseudovirus coated with SARS-CoV-2 Spike protein was used to infect HEK293T/ACE2, and chloroquine was selected as the positive drug. As shown in Fig. 7, the three compounds 5, 10 and 12 in *A. argyi* had a good inhibition effect on pseudovirus invasion within 20 μM , and the inhibition rate reached 54.2385%, 53.7423% and 63.964% at 20 μM , and the cell survival rate was higher than 80% at this concentration. The anti-pseudovirus results of other compounds are shown in Figure S4.

In order to explore the most important domain RBD binding to ACE2 in Spike protein. By SPR analysis of 17 compounds, only C10 and C12 showed strong binding to the RBD of SARS-CoV-2 spike protein, while other sesquiterpenoids such as C3, C8, C13 and C16 showed only weak binding (Figure S5, S6). The K_D values for C10 and C12 binding to SARS-CoV-2-RBD were 181.9 μM and 164.4 μM , respectively. Molecular docking analysis indicated that Compounds 10 and 12 formed hydrogen bonds with Arg403, which led to tight binding to RBD. The α , β -unsaturated γ -lactone structure of C10 and C12 interacted with Glu406 and Arg403 via their ester groups (Fig. 8 (C, D)). Therefore, the unsaturated lactone structure of sesquiterpenes plays a crucial role in their binding

conformation to the RBD protein, with Arg403 serving as the key residue for binding to the spike RBD protein.

3.6. Inhibitory activity of AASs on SARS-CoV-2 M^{Pro}

Main protease (M^{Pro}) is a crucial protease for mediating viral replication and transcription in SARS-CoV-2 (Marinho et al., 2020), making it a potential target for developing drugs against the virus (Fu et al., 2022). To investigate the efficacy of AASs in treating SARS-CoV-2-induced pneumonia, the inhibitory activity of 17 sesquiterpenoids from *A. argyi* against M^{Pro} was analyzed using Ebselen as a positive control drug (Figure S7). The inhibition rate of M^{Pro} on the test compounds showed a clear dose-effect relationship, with the inhibition rate increasing with increasing concentration (Fig. 9(C)). IC_{50} values for Compounds 1, 8, 10, 13, 14, 15, 16 and 17 in *A. argyi* were found to be 24.64 μM , 21.46 μM , 23.17 μM , 35.58 μM , 33.45 μM , 26.34 μM , 35.27 μM , and 8.737 μM .

Based on the inhibition of M^{Pro} activity by sesquiterpenes, the relationship between chemical structure and activity was further analyzed by molecular docking of several sesquiterpenes with strong inhibitory activity (Fig. 10). From the docking results, it is obvious that compounds 15 and 17 are guaiacane-type sesquiterpene lactones, and the O-diol hydroxyl groups at C-3 and C-4 positions of their five-membered rings form a stable hydrogen bond with residue Ser46; Compound 8 also contains the same structure, and its five-membered ring of guaiacane sesquiterpene lactone also has O-diol hydroxyl group, and forms a stable combination with Asn119, so it is considered that this structure is beneficial to interact with M^{Pro} to achieve lower concentration to inhibit its activity. From other docking results, it is also found that residues Thr24 and Thr26 are important groups for sesquiterpenes to bind with M^{Pro} , and unsaturated ketones in sesquiterpenes can form hydrogen bonds with these residues to achieve stability (Fig. 10 (A, C)).

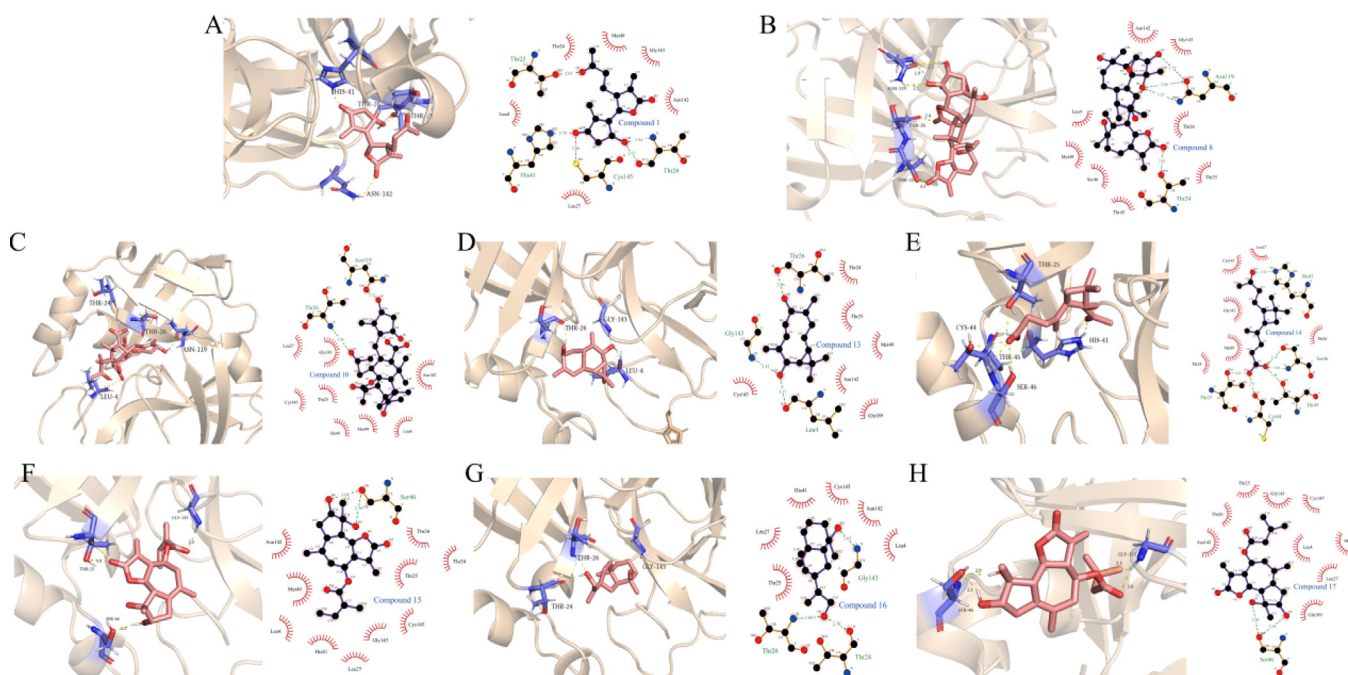


Fig. 10. (A-H) The molecular interaction of SARS-CoV-2 M^{Pro} and Compounds 1, 8, 10, 13, 14, 15, 16 and 17, respectively.

3.7. Inhibition of NO induced by LPS in RAW264.7 cells

Before investigating the inhibitory effect of AASs on NO release in inflammatory RAW264.7 cells *in vitro*, the inhibitory effect of these compounds on cell viability was first studied to screen sesquiterpenes that could exert good anti-inflammatory activity without affecting normal cell growth. Therefore, the cytotoxicity of 17 sesquiterpenoids at 50 μM was studied (Fig. 11 (A)). Compounds 4, 10, 12, 15, 16, 17 showed significant inhibitory effects at the concentration of 50 μM , but Compounds 4, 12, 15, 17 still inhibited normal cell growth at the concentration of 25 μM (Fig. 11 (B)).

The results showed that Compounds 2, 4, 5, 9, 10, 12, 13, 15, 16, and 17 could significantly inhibit the release of NO in RAW264.7 inflammatory model in a concentration-dependent manner, while Compounds 1, 3, 6, 7, 8, 11, and 14 showed a weak inhibitory effect (Figure S6). For example, there are many hydroxyl groups in the structure of C3, C8 and C11, which weakened the lipid solubility of compounds and lead to their weaker inhibitory ability on NO release in RAW264.7 cells than other sesquiterpenes.

Sesquiterpene dimers showed stronger ability to inhibit cellular NO secretion levels compared to monosesquiterpenoids. C10, formed by the polymerization of C1 with another sesquiterpene, showed better inhibition than C1 due to the presence of two active groups despite the destruction of one lactone outer double bond structure. Compound 2, 5, 9, 10, 13, and 16 did not inhibit the growth of RAW264.7 cells at a concentration of 25 μM (Figure S8), while their IC_{50} values for inhibiting the level of NO in RAW264.7 cells were 11.03, 4.415, 6.718, 3.656, 2.605, and 4.189 μM (Fig. 11 (C)), respectively, indicating good activity.

Molecular docking results indicated that C9 and C10 had similar structures, both possessing α , β -unsaturated γ -lactone and α , β -unsaturated ketone functionalities, and displayed comparable binding affinity towards iNOS protein (Fig. 12). However, C10, which had an additional hydroxyl group at the C-8' position, formed a hydrogen bond with amino acid residue Glu263, resulting in a stronger binding force and lower binding energy. Thus, the unsaturated lactone ring and unsaturated ketone functionalities were crucial for the binding conformation of AASs and iNOS protein, while the hydroxyl group in AASs contributed to the binding affinity by reducing the binding energy.

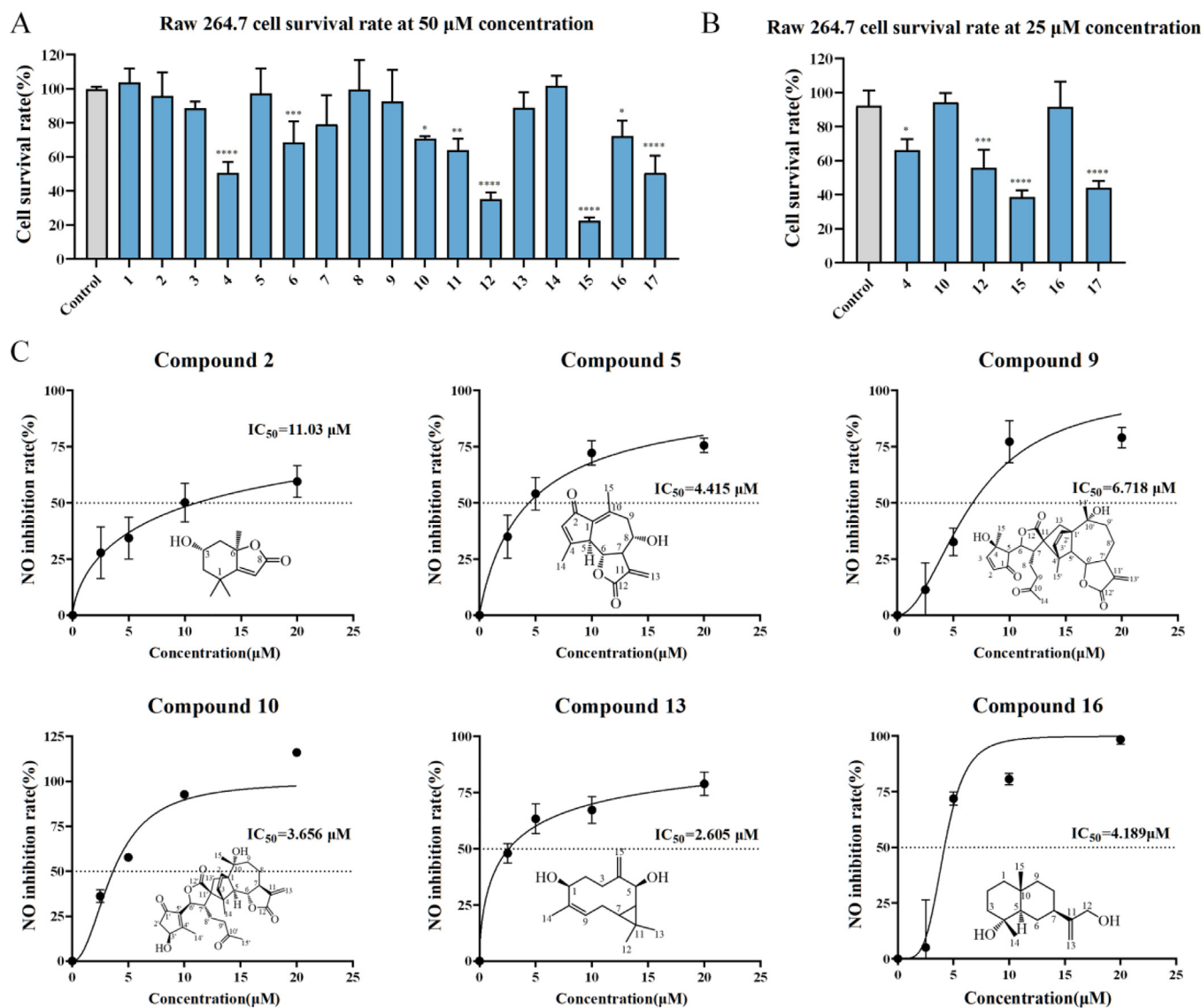


Fig. 11. MTT assay of 17 compounds (50 μM). (B) MTT assay of Compounds 4, 10, 13, 15, 16 and 17 (25 μM). (C) Inhibitory effects of Compounds 2, 5, 9, 10, 13, 16 on NO production in RAW264.7. Results presented as the mean \pm SD of three replicated tests. The GraphPad Prism was used to analyze the results using one-way ANOVA. Note: * $P < 0.05$, ** $P < 0.01$, *** $P < 0.001$, **** $P < 0.0001$.

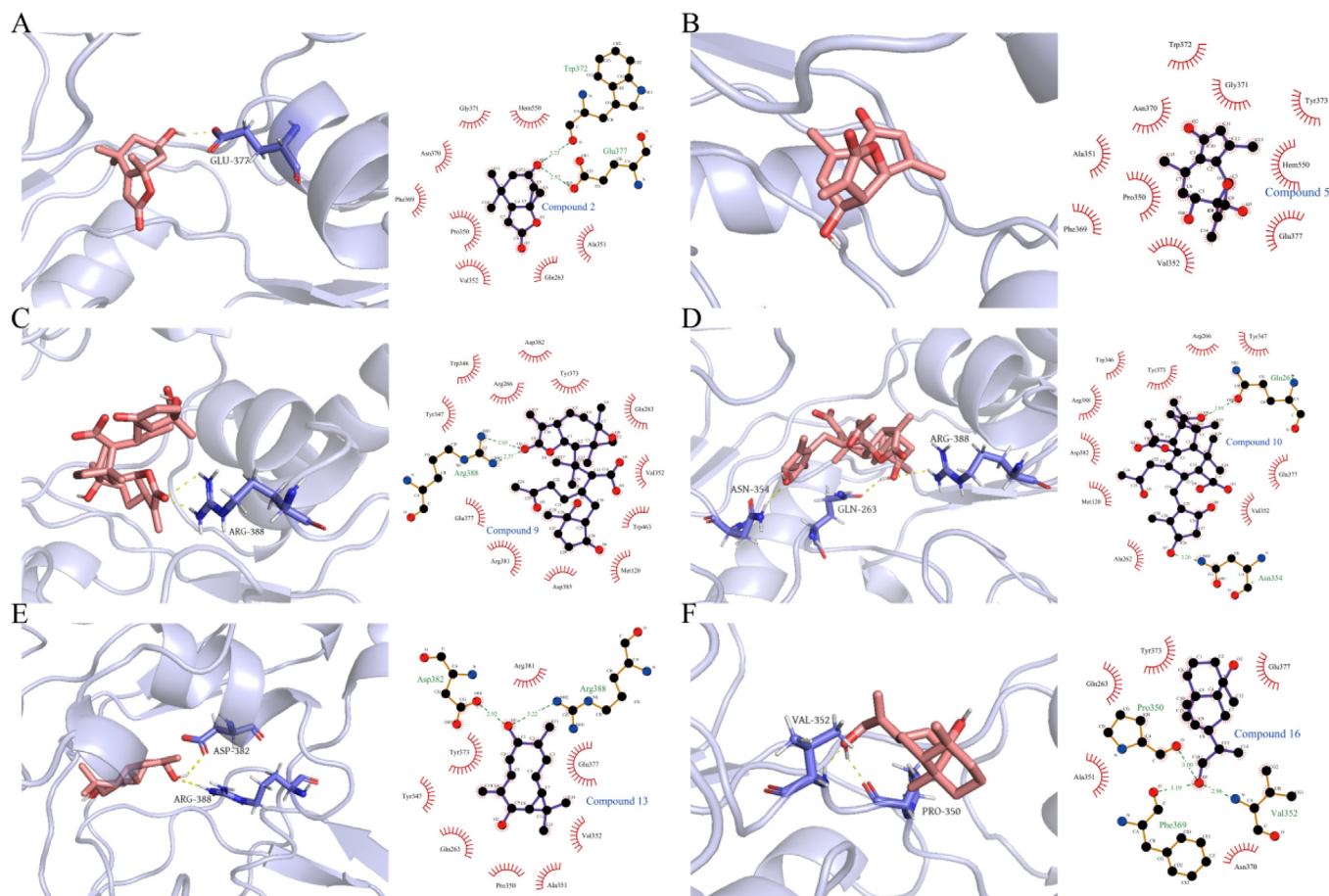


Fig. 12. Interactions of compounds 2, 5, 9, 10, 13, and 16 with iNOS protein, respectively.

3.8. Cytotoxic profiles of the 17 compounds

One of the major problems in the development of medicinal plant-derived drugs is the possible damage to different organs of the human body caused by herbs. To address this issue, in this study, we used human cell lines from three major organs, including liver (HepG2), lung (A549), and intestine (Caco-2), to evaluate the cytotoxicity of these 17 compounds by MTT assay. The results showed that the same compound showed different cytotoxicity in different cell lines. Among them, Compound 10, which had the best combination of anti-Pseudovirus and anti-inflammatory effect, showed obvious toxicity at the concentration of 50 μM , but did not show great toxicity to the three cell lines when the concentration was reduced to 25 μM .

4. Discussion

A. argyi, as a traditional Chinese medicine with a long history of epidemic prevention, has high research value in the context of COVID-19. In this study, *A. argyi* from Tangyin, Henan Province was used to further investigate the relationship between chemical composition, pharmacological effect, chemical structure and activity of sesquiterpenoids, to provide material basis for the research and development of innovative traditional Chinese medicine with a long history of epidemic prevention.

The sesquiterpene fractions of *A. argyi* decoction were extracted by ethanol cold immersion method, and the crude extracts were initially separated by silica gel column chromatography. The

results showed that Fr. 6 and 8 were enriched in sesquiterpenes, and a total of 69 sesquiterpenoids were obtained from the two fractions. This further indicates that *A. argyi* contains abundant sesquiterpene resources and provides a reference for determining the material basis of *A. argyi* medicinal effect and exploring new natural anti-inflammatory lead drugs.

Moreover, through the use of HPLC and chromatographic separation, the monomer compounds of *A. argyi* were isolated and their structures were identified using nuclear magnetic resonance analysis and mass spectrometry. Network pharmacology was employed to explore the potential therapeutic effects of sesquiterpenoids from *A. argyi* in the treatment of COVID-19. By employing a comprehensive approach of identification and prediction, multiple protein targets associated with COVID-19 and SARS-CoV-2 were identified and found to overlap with the AASs. The drug-target-disease map revealed that several AASs exhibited a significant number of cross-protein targets with COVID-19, indicating their potential therapeutic effects in respiratory conditions. The PPI analysis highlighted key proteins involved in the treatment, emphasizing their importance as potential targets for AASs. The functional enrichment analysis provided insights into the molecular functions, cellular components, and biological processes associated with AASs, elucidating their mechanisms of action. Notably, viral-related pathways and cancer-related pathways were prominently identified, suggesting the potential of AASs in treating viral infections and cancer. These findings contribute to the understanding of AASs as potential therapeutic agents for COVID-19 and open avenues for further research and development of targeted therapies (Wang et al., 2018).

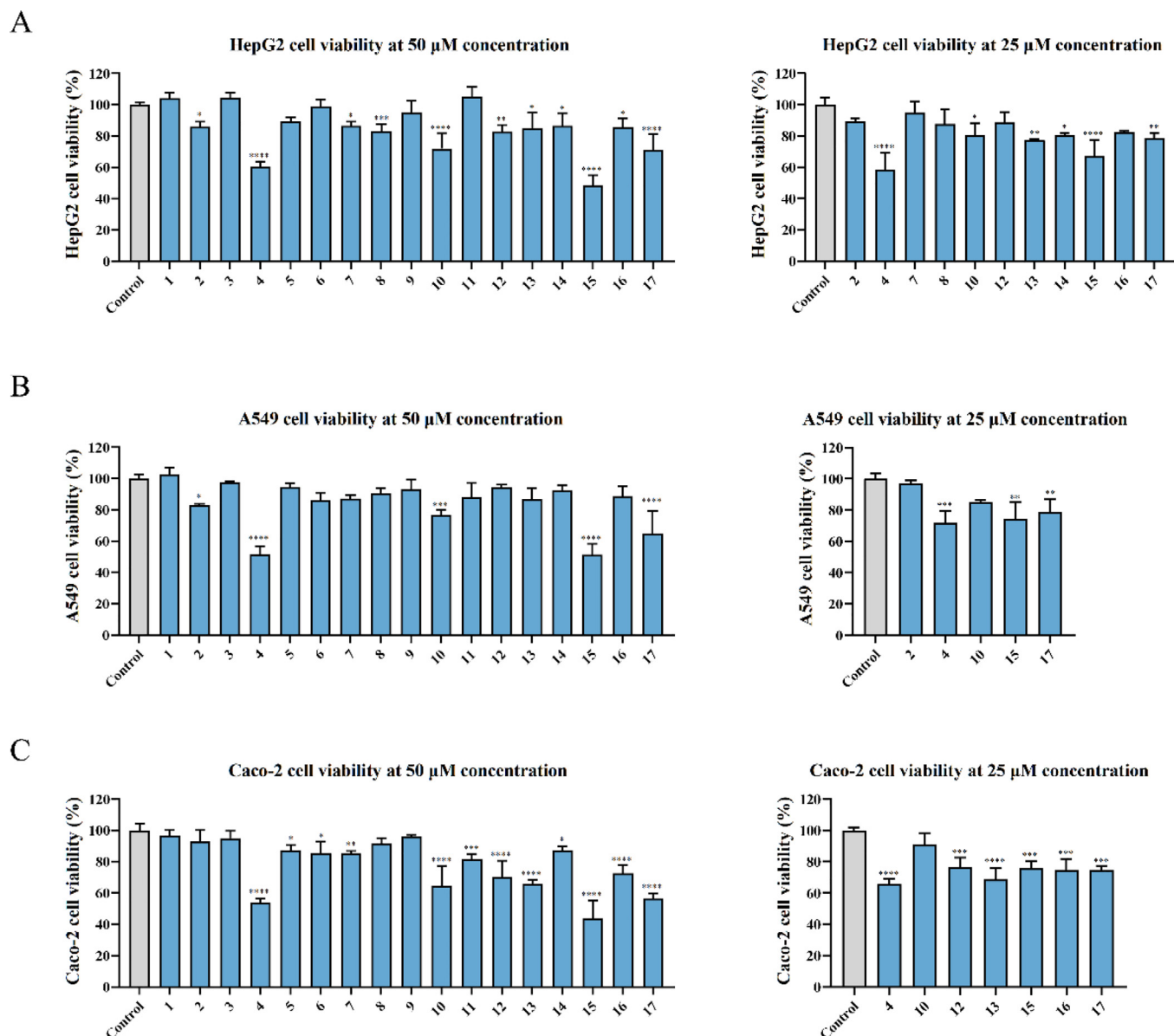


Fig. 13. Cytotoxicity of AASs on three cell lines representing major human organs was assessed by MTT assay after 48 h treatment with (A) liver (HepG2), (B) lung (Calu-3), and (C) intestine (Caco-2) cell lines. All experiments were performed in three biological replicates. The GraphPad Prism was used to analyze the results using one-way ANOVA. Note: * $P < 0.05$, ** $P < 0.01$, *** $P < 0.001$, **** $P < 0.0001$.

Several AASs compounds have shown promising results in inhibiting SARS-CoV-2 infection and reducing inflammation in vitro. Compounds 5, 10, 12 can inhibit the infection of SARS-CoV-2 pseudovirus, and compound 10,12 can form a good binding with RBD in the domain of Spike protein by SPR. For SARS-CoV-2 M^{Pro}, compounds 1, 8, 10, 13, 14, 15, 16 and 17 in AASs could effectively inhibit the activity of M^{Pro}. In addition, compounds 5, 9, 10, 13 and 16 also reduced the anti-inflammatory effect of NO secretion. Finally, the direct analysis of different compounds and protein by molecular docking technology shows that the O-diol hydroxyl group of five-membered ring in guaiacane sesquiterpene lactone can form a stable hydrogen bond with the residue Ser 46 in Mpro, while the structure of α , β -unsaturated- γ -lactone and unsaturated ketone forms a hydrogen bond with the amino acid residue in iNOS protein, achieving a stable binding conformation.

Based on the above in vitro experiments, Compound 10 (Achillinin C) was identified as a promising compound that could inhibit pseudovirus infection and reduce NO secretion to alleviate inflammation. Through a separate systematic pharmacological analysis of

C10, it was found that, as shown in Figure S9, 48 target proteins overlapped with SARS-CoV-2, accounting for more than half of the cross targets between AASs and diseases, and NFKB1 was the most important target protein. The other sesquiterpenes were different, C10 was more concentrated in the KEGG pathway in PD-L1 expression and PD-1 checkpoint pathway in cancer and Coronavirus disease-COVID-19. The present study also found that C10 could effectively inhibit A/Puerto Rico/8/1934 H1N1 influenza virus with an IC₅₀ of 42.29 μM (Zhu et al., 2023), indicating that C10 had good antiviral activity. We believe that these findings lay the foundation for the development of novel natural products with anti-viral and anti-inflammatory effects, and that *A. argyi* could be a promising treatment for this pandemic.

5. Conclusion

In conclusion, this study sheds light on the potential of *A. argyi*, a traditional Chinese medicine, as a source of natural anti-

inflammatory and antiviral compounds in the context of COVID-19. The analysis of sesquiterpenoids obtained from *A. argyi* revealed the presence of abundant sesquiterpene resources and provided a reference for determining the material basis of *A. argyi* medicinal effect and exploring new natural anti-inflammatory lead drugs. Through in vitro testing, several AAS compounds showed promising results for inhibiting SARS-CoV-2 PsV and reducing inflammation. Compound 10 (Achillinin C) was identified as a particularly promising candidate, effectively inhibiting the virus, reducing inflammation, and having no impact on normal cell growth. These findings provide a foundation for the development of new natural medicines for COVID-19 and other inflammatory diseases, as well as contributing to the ongoing search for effective treatments for this pandemic.

Author contributions

The study was designed by Junxia Zheng, Yifei Wang and Zhe Ren. Yujing Huang and YuHui Gan performed the network pharmacology analysis, in vitro experimental studies and molecular docking analysis. Zhilin Huang, Juntao Xie, Zhiyun Xia, Tao Liu and Xiangyu Chen identified sesquiterpenoids of *A. argyi*. Yujing Huang wrote the manuscript. Junxia Zheng, Xiangguang Li, Haibo Zhou and Pinghua Sun edited the manuscript. All data were generated in-house, and no paper mill was used. All authors agree to be accountable for all aspects of work ensuring integrity and accuracy.

Declaration of Competing Interest

The authors declare that they have no known competing financial interests or personal relationships that could have appeared to influence the work reported in this paper.

Acknowledgments

This work was supported by the research grant from the National Natural Science Foundation of China (No. 82073977, 22177039), the General Project of Guangdong Natural Science Foundation (2023A1515011445), the Guangdong joint research fund with enterprises (2022A1515220142), the Guangdong Province Modern Agricultural Industry Technology System Innovation Team Project (Grant No. 2020KJ142 and 2021KJ142) and the Key Research and Development Plan of Guangzhou (Grant No. 202206010008).

Appendix A. Supplementary material

Supplementary data to this article can be found online at <https://doi.org/10.1016/j.arabjc.2023.105298>.

References

- Adekenov, S., Gafurov, N., Turdybekov, K., et al., 1991. Chemical modification of the trans, trans-germacranolide stizolicin synthesis, molecular, and crystal structure of 6 α -acetoxy-13-methoxy-1,10; 4,5-diepoxy-1,5,7 α (H),8,11 β (H)-E, E-germacr-8,12-olide. *Chem. Nat. Compd.* - CHEM. NAT. COMPD. 27, 690–696. <https://doi.org/10.1007/BF00629927>.
- Ahmed, A.A., Gáti, T., Hussein, T.A., et al., 2003. Ligustolide A and B, two novel sesquiterpenes with rare skeletons and three 1,10-seco-guaianolide derivatives from *Achillea ligustica*. *Tetrahedron* 59, 3729–3735. [https://doi.org/10.1016/S0040-4020\(03\)00572-6](https://doi.org/10.1016/S0040-4020(03)00572-6).
- Bu, Q., Yang, M., Yan, X.Y., et al., 2022. Mililatsensols A-C, new records of sarsolenane and capnosane diterpenes from soft coral sarcophyton mililatsensis. *Mar. Drugs* 20. <https://doi.org/10.3390/md20090566>.
- Calixto, N. O., M. S. Cordeiro, T. B. S. Giorno, et al., 2016. Chemical Constituents of *Psychotria nemorosa* Gardner and Antinociceptive Activity. 28, 707–723.
- Cardona, L., Fernández, I., Pedro, J.R., et al., 1992. Polyoxygenated terpenes and cyanogenic glucosides from *Centaurea aspera* var. *subinermis*. *Phytochemistry* 31, 3507–3509. [https://doi.org/10.1016/0031-9422\(92\)83717-D](https://doi.org/10.1016/0031-9422(92)83717-D).

- Chan, C.O., Xie, X.J., Wan, S.W., et al., 2019. Qualitative and quantitative analysis of sesquiterpene lactones in *Centipeda minima* by UPLC-Orbitrap-MS & UPLC-QQQ-MS. *J. Pharm. Biomed. Anal.* 174, 360–366. <https://doi.org/10.1016/j.jpba.2019.05.067>.
- Chen, H., Wu, L., Su, Y., et al., 2022. Inhibitory effects of compounds from *Plumula nelumbinis* on biofilm and quorum sensing against *P. aeruginosa*. *Curr. Microbiol.* 79, 236. <https://doi.org/10.1007/s00284-022-02914-5>.
- Chen, M., Zhang, X.E., 2021. Construction and applications of SARS-CoV-2 pseudoviruses: a mini review. *Int. J. Biol. Sci.* 17, 1574–1580. <https://doi.org/10.7150/ijbs.59184>.
- Dzhalmakhanbetova, R., Rodichev, M., Gatilov, Y., et al., 2009. Epoxidation of sesquiterpene lactones tournefortin and ludartin. *Chem. Nat. Compd.* - CHEM. NAT. COMPD. 45, 503–506. <https://doi.org/10.1007/s10600-009-9399-6>.
- el-Feraly, F. S. and Y. M. Chan, 1978. Isolation and characterization of the sesquiterpene lactones costunolide, parthenolide, costunolide diepoxide, santamarine, and reynosin from *Magnolia grandiflora* L. *Journal of pharmaceutical sciences*. 67, 347–350. <https://doi.org/10.1002/jps.2600670319>.
- Fan, H., Chen, J., Lv, H., et al., 2016. Isolation and identification of terpenoids from chicory roots and their inhibitory activities against yeast α -glucosidase. *Eur. Food Res. Technol.* 243, 1009–1017. <https://doi.org/10.1007/s00217-016-2810-1>.
- Fu, Y., Pan, F., Zhao, L., et al., 2022. Interfering effects on the bioactivities of several key proteins of COVID-19/variants in diabetes by compounds from *Lianqiao* leaves: In silico and in vitro analyses. *Int. J. Biol. Macromol.* 207, 715–729. <https://doi.org/10.1016/j.ijbiomac.2022.03.145>.
- Ganfou, H., Bero, J., Tchinda, A.T., et al., 2012. Antiparasitic activities of two sesquiterpene lactones isolated from *Acanthospermum hispidum* D.C. *J. Ethnopharmacol.* 141, 411–417. <https://doi.org/10.1016/j.jep.2012.03.002>.
- Garlaschelli, L. and G. Vidari, 1989. Synthetic studies on biologically active natural compounds. Part I: Stereospecific transformation of uvidin A into (?)-cinnamodial. 45, 7371–7378.
- Guan, D.D., Chen, L., Liu, K.P., et al., 2021. Progress in the prevention and control of corona virus disease 2019 by moxibustion. *J. Liaoning University TCM* 23, 168–171. <https://doi.org/10.13194/j.issn.1673-842x.2021.03.038>.
- Hajdu, Z., Hohmann, J., Forgo, P., et al., 2014. Antiproliferative activity of *Artemisia asiatica* extract and its constituents on human tumor cell lines. *Planta Med.* 80, 1692–1697. <https://doi.org/10.1055/s-0034-1383146>.
- Hatmal, M.M., Alshaer, W., Al-Hatamleh, M.A.I., et al., 2020. Comprehensive Structural and Molecular Comparison of Spike Proteins of SARS-CoV-2, SARS-CoV and MERS-CoV, and Their Interactions with ACE2. *Cells* 9. <https://doi.org/10.3390/cells9122638>.
- He, Y., Cheng, P., Wang, W., et al., 2018. Rapid investigation and screening of bioactive components in simo decoction via LC-Q-TOF-MS and UF-HPLC-MD methods. *Molecules* 23. <https://doi.org/10.3390/molecules23071792>.
- Hirota, A., Nakagawa, M., Sakai, H., et al., 1984. The biosynthesis of terreacyclic acid A, a novel sesquiterpene antibiotic. *Agric. Biol. Chem.* 48, 835–837. <https://doi.org/10.1080/00021369.1984.10866231>.
- Hong, C., Chang, C., Zhang, H., et al., 2019. Identification and characterization of polyphenols in different varieties of *Camellia oleifera* seed cakes by UPLC-QTOF-MS. *Food Res. Int.* 126. <https://doi.org/10.1016/j.foodres.2019.108614>.
- Jimenez-Gonzalez, A., Quispe, C., Borquez, J., et al., 2018. UHPLC-ESI-ORBITRAP-MS analysis of the native Mapuche medicinal plant palo negro (*Leptocarpha rivularis* DC. - Asteraceae) and evaluation of its antioxidant and cholinesterase inhibitory properties. *J. Enzyme Inhib. Med. Chem.* 33, 936–944. <https://doi.org/10.1080/14756366.2018.1466880>.
- Kallo, G., Kunkli, B., Gyori, Z., et al., 2020. Compounds with antiviral, anti-inflammatory and anticancer activity identified in wine from Hungary's Tokaj Region via high resolution mass spectrometry and bioinformatics analyses. *Int. J. Mol. Sci.* 21. <https://doi.org/10.3390/ijms21249547>.
- Kanawati, B., Herrmann, F., Joniec, S., et al., 2008. Mass spectrometric characterization of beta-caryophyllene ozonolysis products in the aerosol studied using an electrospray triple quadrupole and time-of-flight analyzer hybrid system and density functional theory. *Rapid Commun. Mass Spectrom.* 22, 165–186. <https://doi.org/10.1002/rcm.3340>.
- Lee, J. T., Q. Yang, A. Gribenko, et al., 2022. Genetic Surveillance of SARS-CoV-2 M (pro) Reveals High Sequence and Structural Conservation Prior to the Introduction of Protease Inhibitor Paxlovid. *mBio.* 13, e0086922. <https://doi.org/10.1128/mbio.00869-22>.
- Li, H., Cheng, C., Shi, S., et al., 2022. Identification, optimization, and biological evaluation of 3-O- β -chacotriosyl ursolic acid derivatives as novel SARS-CoV-2 entry inhibitors by targeting the prefusion state of spike protein. *Eur. J. Med. Chem.* 238. <https://doi.org/10.1016/j.ejmech.2022.114426>.
- Li, Q., Liang, X., Zhao, L., et al., 2017. UPLC-Q-exactive orbitrap/MS-based lipidomics approach to characterize lipid extracts from bee pollen and their in vitro anti-inflammatory properties. *J. Agric. Food Chem.* 65, 6848–6860. <https://doi.org/10.1021/acs.jafc.7b02285>.
- Li, L., Liu, H., Tang, C., et al., 2017. Cytotoxic sesquiterpene lactones from *Artemisia anomala*. *Phytochem. Lett.* 20, 177–180. <https://doi.org/10.1016/j.phytol.2017.04.038>.
- Li, P., Su, W., Xie, C., et al., 2015. Rapid identification and simultaneous quantification of multiple constituents in Nao-Shuan-tong capsule by ultra-fast liquid chromatography/diode-array detector/quadrupole time-of-flight tandem mass spectrometry. *J. Chromatogr. Sci.* 53, 886–897. <https://doi.org/10.1093/chromsci/bmu137>.

- Li, Y., Wang, Y., Li, T., et al., 2023. Sesquiterpene from *Artemisia argyi* seed extracts: A new anti-acute peritonitis agent that suppresses the MAPK pathway and promotes autophagy. *Inflammopharmacology*. <https://doi.org/10.1007/s10787-023-01297-8>.
- Li, Y.T., Yang, C., Wu, Y., et al., 2021. Axial chiral binaphthoquinone and perylenequinones from the stromata of *Hypocrella bambusae* Are SARS-CoV-2 entry inhibitors. *J. Nat. Prod.* 84, 436–443. <https://doi.org/10.1021/acs.jnatprod.0c01136>.
- Lin, P., Wang, Q., Liu, Y., et al., 2020. Characterization of chemical profile and quantification of representative components of DanLou tablet, a traditional Chinese medicine prescription, by UHPLC-Q/TOF-MS combined with UHPLC-TQ-MS. *J. Pharm. Biomed. Anal.* 180., <https://doi.org/10.1016/j.jpba.2019.113070> 113070.
- Liu, X.Y., Chang, Y.L., Wang, X.H., et al., 2021. An integrated approach to uncover anti-tumor active materials of *Curcuma Rhizoma-Sparganii Rhizoma* based on spectrum-effect relationship, molecular docking, and ADME evaluation. *J. Ethnopharmacol.* 280., <https://doi.org/10.1016/j.jep.2021.114439> 114439.
- Liu, H., Edrada-Ebel, R., Ebel, R., et al., 2009. Drimane sesquiterpenoids from the fungus *Aspergillus ustus* isolated from the marine sponge *Suberites domuncula*. *J. Nat. Prod.* 72, 1585–1588. <https://doi.org/10.1021/np900220r>.
- Liu, Y., He, Y., Wang, F., et al., 2021. From longevity grass to contemporary soft gold: Explore the chemical constituents, pharmacology, and toxicology of *Artemisia argyi* H.Lév. & vaniot essential oil. *J. Ethnopharmacol.* 279., <https://doi.org/10.1016/j.jep.2021.114404> 114404.
- Liu, M.L., Liu, M., Zhong, H., et al., 2020. Significance and operation mode of moxibustion intervention for the group under quarantine after close contact with COVID-19. *Zhongguo zhen jiu = Chinese Acupunct. Moxibust.* 40, 457–461. <https://doi.org/10.13703/j.0255-2930.20200224-k0004>.
- Liu, M., Wang, J., Wan, X., et al., 2023. Discovery and structural optimization of 3-O- β -Chacotriosyl betulonic acid saponins as potent fusion inhibitors of Omicron virus infections. *Bioorg. Chem.* 131., <https://doi.org/10.1016/j.bioorg.2022.106316> 106316.
- Lokhande, K.B., Kale, A., Shahakar, B., et al., 2023. Terpenoid phytochemicals from mangrove plant *Xylocarpus moluccensis* as possible inhibitors against SARS-CoV-2: In silico strategy. *Comput. Biol. Chem.* 106., <https://doi.org/10.1016/j.compbiolchem.2023.107912> 107912.
- Lou, Y., Zhao, F., He, H., et al., 2009. Guaiane-type sesquiterpenes from *Curcuma wenyujin* and their inhibitory effects on nitric oxide production. *J. Asian Nat. Prod. Res.* 11, 737–747. <https://doi.org/10.1080/10286020903042358>.
- Maldonado, E., Mendoza, G., cárdenas, J., et al., 1985. Sesquiterpene lactones from *Parthenium tomentosum*. *Phytochemistry* 24, 2981–2985. [https://doi.org/10.1016/0031-9422\(85\)80040-6](https://doi.org/10.1016/0031-9422(85)80040-6).
- Marinho, E.M., Batista de Andrade Neto, J., Silva, J., et al., 2020. Virtual screening based on molecular docking of possible inhibitors of Covid-19 main protease. *Microb. Pathog.* 148., <https://doi.org/10.1016/j.micpath.2020.104365> 104365.
- Masih, A., Agnihotri, A.K., Srivastava, J.K., et al., 2021. Discovery of novel pyrazole derivatives as a potent anti-inflammatory agent in RAW264.7 cells via inhibition of NF- κ B for possible benefit against SARS-CoV-2. *J. Biochem. Mol. Toxicol.* 35, e22656.
- Mathon, C., Duret, M., Kohler, M., et al., 2013. Multi-targeted screening of botanicals in food supplements by liquid chromatography with tandem mass spectrometry. *Food Chem.* 138, 709–717. <https://doi.org/10.1016/j.foodchem.2012.10.091>.
- Michalska, K., K. Pieron and A. Stojakowska, 2018. Sesquiterpene Lactones and Phenolics from Roots of *Leontodon hispidus* subsp. *hispidus*. 13, 1934578X1801300403. <https://doi.org/10.1177/1934578x1801300403>.
- Ming, J., Liu, W., Wu, H., et al., 2021. The active ingredients and mechanisms of Longchai Jiangxue Formula in treating PV, based on UPLC-Q-TOF-MS/MS, systematic pharmacology, and molecular biology validation. *Biomed. Pharmacother.* 140., <https://doi.org/10.1016/j.biopha.2021.111767> 111767.
- Muhseen, Z.T., Hameed, A.R., Al-Hasani, H.M.H., et al., 2020. Promising terpenes as SARS-CoV-2 spike receptor-binding domain (RBD) attachment inhibitors to the human ACE2 receptor: Integrated computational approach. *J. Mol. Liq.* 320., <https://doi.org/10.1016/j.molliq.2020.114493> 114493.
- Nielsen, K.F., Mansson, M., Rank, C., et al., 2011. Dereplication of microbial natural products by LC-DAD-TOFMS. *J. Nat. Prod.* 74, 2338–2348. <https://doi.org/10.1021/np200254t>.
- Öksüz, S., 1990. Sesquiterpenoids and other constituents from *Tanacetum cilicium*. *Phytochemistry* 29, 887–890. [https://doi.org/10.1016/0031-9422\(90\)80039-J](https://doi.org/10.1016/0031-9422(90)80039-J).
- Park, H.J., Cho, J.G., Baek, Y.S., et al., 2016. Identification of bitter components from *Artemisia princeps* Pamp. *Food Sci. Biotechnol.* 25, 27–32. <https://doi.org/10.1007/s10068-016-0004-z>.
- Park, M. Y., S. E. Ha, H. H. Kim, et al., 2022. Scutellarein Inhibits LPS-Induced Inflammation through NF- κ B/MAPKs Signaling Pathway in RAW264.7 Cells. *Molecules* (Basel, Switzerland). 27, <https://doi.org/10.3390/molecules27123782>.
- Perez-Souto, N., Lynch, R.J., Measures, G., et al., 1992. Use of high-performance liquid chromatographic peak deconvolution and peak labelling to identify antiparasitic components in plant extracts. *J. Chromatogr.* 593, 209–215. [https://doi.org/10.1016/0021-9673\(92\)80288-6](https://doi.org/10.1016/0021-9673(92)80288-6).
- Ranasinghe, A., Sweatlock, J., Cooks, R., 1993. A rapid screening method for artemisinin and its congeners using Ms/Ms: Search for new analogues in *Artemisia annua*. *J. Nat. Prod.* 56, 552–563. <https://doi.org/10.1021/np50094a016>.
- Razgonova, M., Zakharenko, A., Ercisli, S., et al., 2020. Comparative analysis of far East Sikhotinsky *Rhododendron* (*Rh. sichotense*) and East Siberian *Rhododendron* (*Rh. adamsii*) using supercritical CO₂-extraction and HPLC-ESI-MS/MS spectrometry. *Molecules* 25, <https://doi.org/10.3390/molecules25173774>.
- Ruangrungring, N., Kasiwong, S., Likhithitayawuid, K., et al., 1989. Constituents of *Grangea maderaspatana*. A New Eudesmanolide. *J. Nat. Prod. - J. NAT. PROD.* 52, 130–134. <https://doi.org/10.1021/np50061a016>.
- Rustaiyan, A., Habibi, Z., Saberi, M., et al., 1991. A nor-guaianolide and A glaucolide-like eudesmanolide from *Pulicaria undulata*. *Phytochemistry* 30, 2405–2406. [https://doi.org/10.1016/0031-9422\(91\)83662-5](https://doi.org/10.1016/0031-9422(91)83662-5).
- Sa-Ngiamsumtorn, K., Suksatu, A., Pewklaiang, Y., et al., 2021. Anti-SARS-CoV-2 activity of *andrographis paniculata* extract and its major component andrographolide in human lung epithelial cells and cytotoxicity evaluation in major organ cell representatives. *J. Nat. Prod.* 84, 1261–1270. <https://doi.org/10.1021/acs.jnatprod.0c01324>.
- Shao, Z., Li, L., Zheng, Y., et al., 2022. Anti-inflammatory sesquiterpenoid dimers from *Artemisia atrovirens*. *Fitoterapia* 159., <https://doi.org/10.1016/j.fitote.2022.105199> 105199.
- Sharifi-Rad, J., J. Herrera-Bravo, P. Semwal, et al., 2022. *Artemisia* spp.: An Update on Its Chemical Composition, Pharmacological and Toxicological Profiles. *Oxidative medicine and cellular longevity*. 2022, 5628601. <https://doi.org/10.1155/2022/5628601>.
- Sheng, N., Zheng, H., Xiao, Y., et al., 2017. Chiral separation and chemical profile of Dengzhan Shengmai by integrating comprehensive with multiple heart-cutting two-dimensional liquid chromatography coupled with quadrupole time-of-flight mass spectrometry. *J. Chromatogr. A* 1517, 97–107. <https://doi.org/10.1016/j.chroma.2017.08.037>.
- Skaltsa, H., D. Lazari, C. Panagouleas, et al., 2001. ChemInform Abstract: Sesquiterpene Lactones from *Centaurea thessala* and *Centaurea attica*. Antifungal Activity. *Phytochemistry*. 55, 903–908. [https://doi.org/10.1016/S0031-9422\(00\)00254-5](https://doi.org/10.1016/S0031-9422(00)00254-5).
- Song, A.R., Sun, X.L., Kong, C., et al., 2014. Discovery of a new sesquiterpenoid from *Pheillinus ignarius* with antiviral activity against influenza virus. *Arch. Virol* 159, 753–760. <https://doi.org/10.1007/s00705-013-1857-6>.
- Sugawara, F., Hallock, Y.F., Bunkers, G.D., et al., 1993. Phytoactive eremophilanes produced by the weed pathogen *Drechslera gigantea*. *Biosci. Biotech. Bioch.* 57, 236–239. <https://doi.org/10.1271/bbb.57.236>.
- Sumarah, M.W., Puniani, E., Sorensen, D., et al., 2010. Secondary metabolites from anti-insect extracts of endophytic fungi isolated from *Picea rubens*. *Phytochemistry* 71, 760–765. <https://doi.org/10.1016/j.phytochem.2010.01.015>.
- Talzhonov, N., Rodichev, M., Raldugin, V., et al., 2007. Tournefortin, a novel eudesmanolide from *Artemisia tournefortiana*. *Chem. Nat. Compd. - CHEM. NAT. COMPD.* 43, 555–557. <https://doi.org/10.1007/s10600-007-0190-2>.
- Tine, Y., Diop, A., Diatta, W., et al., 2017. Chemical diversity and antimicrobial activity of volatile compounds from *Zanthoxylum zanthoxyloides* Lam. according to compound classes, plant organs and senegalese sample locations. *Chem. Biodivers.* 14. <https://doi.org/10.1002/cbdv.201600125>.
- Triana, J., López, M., Rico, M., et al., 2003. Sesquiterpenoid derivatives from *gonospermum elegans* and their cytotoxic activity for HL-60 human promyelocytic cells. *J. Nat. Prod.* 66, 943–948. <https://doi.org/10.1021/np200390y>.
- Vegh, K., Riethmuller, E., Hosszu, L., et al., 2018. Three newly identified lipophilic flavonoids in *Tanacetum parthenium* supercritical fluid extract penetrating the Blood-Brain Barrier. *J. Pharm. Biomed. Anal.* 149, 488–493. <https://doi.org/10.1016/j.jpba.2017.11.029>.
- Velten, R., Klostermeyer, D., Steffan, B., et al., 1994. The mniopetals, new inhibitors of reverse transcriptases from a Mniopetalum species (*Basidiomycetes*) - II: Structure elucidation. *J. Antibiot.* 47, 1017–1024. <https://doi.org/10.7164/antibiotics.47.1017>.
- V'Kovski, P., Kratzel, A., Steiner, S., et al., 2021. Coronavirus biology and replication: implications for SARS-CoV-2. *Nat. Rev. Microbiol.* 19, 155–170. <https://doi.org/10.1038/s41579-020-00468-6>.
- Wang, P. H., J. Xu and M. Y. Wu, 1993. [Chemical constituents of ragweed (*Ambrosia artemisiifolia* L.)]. *Zhongguo Zhong Yao Za Zhi*. 18, 164–166, 191.
- Wang, F., Huang, S., Chen, Q., et al., 2020. Chemical characterisation and quantification of the major constituents in the Chinese herbal formula Jian-Pi-Yi-Shen pill by UPLC-Q-TOF-MS/MS and HPLC-QQQ-MS/MS. *Phytochem. Anal* 31, 915–929. <https://doi.org/10.1002/pca.2963>.
- Wang, L., Pu, X., Nie, X., et al., 2021. Integrated serum pharmacochimistry and network pharmacological analysis used to explore possible anti-rheumatoid arthritis mechanisms of the Shentong-Zhuyu decoction. *J. Ethnopharmacol.* 273., <https://doi.org/10.1016/j.jep.2021.113988> 113988.
- Wang, K., Tian, J., Li, Y., et al., 2021. Identification of components in *citri sarcodactylis fructus* from different origins via UPLC-Q-Exactive Orbitrap/MS. *ACS Omega* 6, 17045–17057. <https://doi.org/10.1021/acsomega.1c02124>.
- Wang, L.-J., Xiong, J., Liu, S.-T., et al., 2014. ChemInform abstract: Sesquiterpenoids from *Chloranthus henryi* and their antineuroinflammatory activities. *Chem. Biodivers.* 11, 919–928. <https://doi.org/10.1002/cbdv.201300283>.
- Wang, Z.L., Zhang, J., Du, D.Q., et al., 2020. Adjuvant therapeutic effects of moxibustion on COVID-19: A protocol for systematic review and meta-analysis. *Medicine* (Baltimore) 99, e23198. <https://doi.org/10.1097/md.00000000000023198>.
- Wang, L.X., Zhao, Q., Zhang, Y., et al., 2022. Network pharmacology and pharmacological evaluation for deciphering novel indication of Sishen Wan in insomnia treatment. *Phytomed. : Int. J. Phytother. Phytopharmacol.* 108., <https://doi.org/10.1016/j.phymed.2022.154500> 154500.

- Wang, B., Zhou, R.R., Tang, S.H., 2018. Study on relevance mining of "core drug action target" in Dictionary of Traditional Chinese Medicine Prescriptions. *Zhongguo Zhong Yao Za Zhi* 43, 3919–3926. <https://doi.org/10.19540/j.cnki.cjmm.20180710.002>.
- Werner, I., S. Glasl, A. Presser, et al., 2003. Sesquiterpenes from *Achillea pannonica* Scheele. *Zeitschrift für Naturforschung. C, Journal of biosciences*. 58, 303–307. <https://doi.org/10.1515/znc-2003-5-601>.
- Wu, Z., Chen, X., Ni, W., et al., 2021. The inhibition of Mpro, the primary protease of COVID-19, by *Poria cocos* and its active compounds: a network pharmacology and molecular docking study. *RSC Adv.* 11, 11821–11843. <https://doi.org/10.1039/d0ra07035a>.
- Wu, Q.G., Huang, L.Y., Fan, M.H., et al., 2023. Anti-inflammatory activities of monoterpene and sesquiterpene glycosides from the aqueous extract of *Artemisia annua* L. *Chem. Biodivers.* 20, e202201237.
- Wu, Q.Y., Wong, Z.C., Wang, C., et al., 2019. Isoorientin derived from *Gentiana veitchiorum* Hemsl. flowers inhibits melanogenesis by down-regulating MITF-induced tyrosinase expression. *Phytomed. : Int. J. Phytother. Phytopharmacol.* 57, 129–136. <https://doi.org/10.1016/j.phymed.2018.12.006>.
- Xia, Z., Z. Huang, T. Liu, et al., 2023. Isolation and structural identification of sesquiterpenes from *Artemisia argyi* H. Lév. & Vaniot. *Chinese Journal of Medicinal Chemistry*. 2023,33(02).
- Xia, S., Liu, M., Wang, C., et al., 2020. Inhibition of SARS-CoV-2 (previously 2019-nCoV) infection by a highly potent pan-coronavirus fusion inhibitor targeting its spike protein that harbors a high capacity to mediate membrane fusion. *Cell Res.* 30, 343–355. <https://doi.org/10.1038/s41422-020-0305-x>.
- Xiao, Y., Wu, X., Yao, X., et al., 2021. Metabolite profiling, antioxidant and alpha-glucosidase inhibitory activities of buckwheat processed by solid-state fermentation with *Eurotium cristatum* YL-1. *Food Res. Int.* 143. <https://doi.org/10.1016/j.foodres.2021.110262>.
- Xu, J., Pan, L.J., Jia, C.S., 2020. Exploration on the feasibility of moxibustion in prevention and treatment of COVID-19 from the perspective of modern medical mechanism. *World J. Acupunct.-Moxibust.* 30, 81–84. <https://doi.org/10.1016/j.wjam.2020.06.001>.
- Xu, K., Zhou, Q., Li, X.Q., et al., 2020. Cadinane- and drimane-type sesquiterpenoids produced by *Paecilomyces* sp. TE-540, an endophyte from *Nicotiana tabacum* L., are acetylcholinesterase inhibitors. *Bioorg. Chem.* 104. <https://doi.org/10.1016/j.bioorg.2020.104252>.
- Xue, G.M., Li, X.Q., Chen, C., et al., 2018. Highly oxidized guaianolide sesquiterpenoids with potential anti-inflammatory activity from *Chrysanthemum indicum*. *J. Nat. Prod.* 81, 378–386. <https://doi.org/10.1021/acs.jnatprod.7b00867>.
- Xue, G.M., Zhu, D.R., Han, C., et al., 2019. Artemisianins A-D, new stereoisomers of seco-guaianolide involved heterodimeric [4+2] adducts from *Artemisia argyi* induce apoptosis via enhancement of endoplasmic reticulum stress. *Bioorg. Chem.* 84, 295–301. <https://doi.org/10.1016/j.bioorg.2018.11.013>.
- Xue, G.M., Xue, J.F., Zhao, C.G., et al., 2021. Sesquiterpenoids from *Artemisia argyi* and their NO production inhibitory activity in RAW264.7 cells. *Nat. Prod. Res.* 35, 2887–2894. <https://doi.org/10.1080/14786419.2019.1680665>.
- Yalamançılı, C., Manda, V.K., Chittiboyina, A.G., et al., 2017. Utilizing Ayurvedic literature for the identification of novel phytochemical inhibitors of botulinum neurotoxin A. *J. Ethnopharmacol.* 197, 211–217. <https://doi.org/10.1016/j.jep.2016.07.069>.
- Yamakawa, K., Satoh, T., Ohba, N., et al., 1981. Studies on the terpenoids and related alicyclic compounds—XXII Part XXI. K. Yamakawa, K. Nishitani, A. Murakami and Y. Iitaka, *Chem. Pharm. Bull. Tokyo*, 28, 3244 (1980).: Stereochemical study on the angular hydroxylation of polycyclic ketones using benzeneseleninic anhydride. *Tetrahedron* 37, 473–479. [https://doi.org/10.1016/S0040-4020\(01\)92418-4](https://doi.org/10.1016/S0040-4020(01)92418-4).
- Yan, S., Li, S., Wu, W., et al., 2011. Terpenoid and phenolic metabolites from the fungus *Xylaria* sp. associated with termite nests. *Chem. Biodivers.* 8, 1689–1700. <https://doi.org/10.1002/cbdv.201100026>.
- Yang, Y., Li, Y., Liu, X., 2021b. Ancient literature and modern research on prevention and treatment of epidemic diseases with moxibustion. *Trad. Chinese Med. J.* 20, 39–42. <https://doi.org/10.14046/j.cnki.zyytb2002.2021.06.012>.
- Yang, L., Pei, R.J., Li, H., et al., 2021a. Identification of SARS-CoV-2 entry inhibitors among already approved drugs. *Acta Pharmacol. Sin.* 42, 1347–1353. <https://doi.org/10.1038/s41401-020-00556-6>.
- Ye, M., Luo, G., Ye, D., et al., 2021. Network pharmacology, molecular docking integrated surface plasmon resonance technology reveals the mechanism of Toujie Quwen Granules against coronavirus disease 2019 pneumonia. *Phytomed. : Int. J. Phytother. Phytopharmacol.* 85. <https://doi.org/10.1016/j.phymed.2020.153401>.
- Yi, Y., Li, J., Lai, X., et al., 2022. Natural triterpenoids from licorice potently inhibit SARS-CoV-2 infection. *J. Adv. Res.* 36, 201–210. <https://doi.org/10.1016/j.jare.2021.11.012>.
- Zdero, C., Bohlmann, F., 1990. Sesquiterpene lactones from *Dicoma* species. *Phytochemistry* 29, 183–187. [https://doi.org/10.1016/0031-9422\(90\)89034-7](https://doi.org/10.1016/0031-9422(90)89034-7).
- Zdero, C., Bohlmann, F., King, R.M., et al., 1986. Pyrone derivatives from *Podolepis hieracioides* and sesquiterpene acids from *Cassia longifolia*. *Phytochemistry* 26, 187–190. [https://doi.org/10.1016/S0031-9422\(00\)81508-3](https://doi.org/10.1016/S0031-9422(00)81508-3).
- Zeng, K.W., Wang, S., Dong, X., et al., 2014. Sesquiterpene dimer (DSF-52) from *Artemisia argyi* inhibits microglia-mediated neuroinflammation via suppression of NF-κB, JNK/p38 MAPKs and Jak2/Stat3 signaling pathways. *Phytomed. : Int. J. Phytother. Phytopharmacol.* 21, 298–306. <https://doi.org/10.1016/j.phymed.2013.08.016>.
- Zhu, D., Yuan, J., Yue, Q., et al., 2023. Building block extractor: An MS/MS data mining tool for targeted discovery of natural products with specified features. *Anal. Chem.* 95, 10939–10946. <https://doi.org/10.1021/acs.analchem.3c00744>.